

<https://doi.org/10.5800/GT-2019-10-2-0423>

AN OVERVIEW OF CLASTIC DIKES: SIGNIFICANCE FOR EARTHQUAKE STUDY

O. V. Lunina

Institute of the Earth's Crust, Siberian Branch of RAS, Irkutsk, Russia

Abstract: Clastic dikes are often the only evidence of past disasters in poorly exposed areas and therefore their findings are extremely important for earthquake study. However, the variety of their origins greatly complicates the use of clastic dikes to assess the seismic hazards within the manifold environments. This paper systematizes main triggers, formation mechanisms and some matching indicative features of tabular and cylindrical bodies with an emphasis on the importance of revealing the injection dikes formed by fluidized injection of clastic material into the host sedimentary layers (from the bottom upwards) and associated with overpressure buildup and hydraulic fracturing. Based on the revision of known seismic liquefaction features and specific descriptions of the injection dikes, this overview defines 12 general and 12 individual geological and structural criteria (for study in sectional view), which make it possible to establish confidently the earthquake origin of the dikes caused by fluidization from seismic liquefaction. In addition, ground penetrating radar data correlating with trenching suggest indicative searching criteria of the injection dikes on radargrams, namely: a pipe-shaped anomaly or a composite anomaly combining a tubular form in the lower part with an isometric – in the upper [i]; relatively high values of unipolar positive echoes on the trace of GPR signal [ii]; an occurrence of the same anomaly on adjacent parallel profiles located the first tens of meters apart [iii]; and stratigraphic disruptions of the radar events on the background of their continuous horizontal position [iv]. Finally, the paper illustrates that the clastic dikes can be successfully applied to determine the age and the recurrence interval, the epicenter location and a lower-bound magnitude/intensity of paleoearthquakes, thus providing geological data for seismic hazard assessments in the regions, in which unconsolidated deposits capable to liquefaction are common.

Key words: clastic dike; liquefaction; earthquake; criterion; ground-penetrating radar; paleoseismic reconstruction

RESEARCH ARTICLE

Received: September 12, 2018

Revised: March 14, 2019

Accepted: April 3, 2019

For citation: Lunina O.V., 2019. An overview of clastic dikes: significance for earthquake study. *Geodynamics & Tectonophysics* 10 (2), 483–506. doi:10.5800/GT-2019-10-2-0423.

КЛАСТИЧЕСКИЕ ДАЙКИ И ИХ ЗНАЧЕНИЕ ДЛЯ ИЗУЧЕНИЯ ЗЕМЛЕТРЯСЕНИЙ

О. В. Лунина

Институт земной коры СО РАН, Иркутск, Россия

Аннотация: Кластические дайки часто являются единственным свидетельством прошлых стихийных бедствий на слабообнаженных территориях, поэтому их находки исключительно важны, в том числе и для изучения землетрясений. Однако процессы, которые приводят к их формированию, многообразны, что сильно осложняет использование кластических даек для оценки сейсмической опасности в разных окружающих обстановках. Настоящая статья систематизирует главные триггеры, механизмы формирования и некоторые характерные для них признаки пластинообразных и цилиндрических геологических тел с особым акцентом на важность выявления инъекционных даек, образование которых происходит в результате внедрения разжиженного материала снизу вверх в осадочные слои вследствие действия аномально высокого порового давления и разрывообразования. На основе ревизии известных признаков сейсмического разжижения и конкретных описаний инъекционных даек сформулировано 12 общих и 12 индивидуальных геологоструктурных критериев, применение которых непосредственно на обнажении позволяет достаточно точно установить их происхождение, связанное с землетрясениями, и исключить несейсмогенные триггеры. В дополнение по георадиолокационным данным, заверенным прямыми наблюдениями в канавах, выделено четыре поисковых признака, которые позволяют предварительно идентифицировать инъекционные дайки на радарограммах: трубообразная форма аномалии или сочетание трубообразной формы в нижней части с изометричной – в верхней [i]; относительно высокие значения однополярных положительных амплитуд сигналов [ii]; наличие одной и той же аномалии на соседних параллельных профилях, расположенных в пределах первых десятков метров друг от друга [iii]; стратиграфические разрывы осей синфазности на фоне их непрерывного субгоризонтального положения (iv). Статья иллюстрирует возможности использования кластических даек для палеосейсмогеологических реконструкций, а именно для определения возраста и интервала повторяемости землетрясений, местоположения эпицентра, минимально возможной магнитуды и макросейсмической интенсивности по шкале MSK-64. Таким образом, кластические дайки могут обеспечивать базовые геологические данные для оценки сейсмической опасности регионов, в которых рыхлые отложения, способные к разжижению, широко распространены.

Ключевые слова: кластическая дайка; разжижение; землетрясение; критерий; георадиолокация; палеосейсмическая реконструкция

1. INTRODUCTION

The clastic dikes are tabular geological bodies filled with sedimentary material and cutting across sedimentary strata or other rock types. They were first found in the vicinity of St. Petersburg [Srtangways, 1821] and later in the east of Argentina [Darwin, 1846], and since then, for almost 200 years, specialists have been describing these structures, arguing about their origins and trying to use the clastic dikes for unraveling the secrets of the geological record [Newsom, 1903; Borchardt, Mace, 1992; Larsen, Mangerud, 1992; Sims, Garvin, 1995; Obermeier, 1996, 1998; Vanneste et al., 1999; Obermeier et al., 2005; Bezerra et al., 2001; Jolly, Lonergan, 2002; Jonk et al., 2003; van Vliet-Lanoë et al., 2004; Castilla, Audemard, 2007; Porat et al., 2007; Goździk, van Loon, 2007; Moretti, Sabato, 2007; Levi et al., 2006, 2009, 2011; Chen et al., 2009; Deev et al., 2009, 2015; Rusakov, Nikonov, 2010; Rogozhin, 2012; Talwani et al., 2011; van Loon, Maulik, 2011; Cooley, 2011; Novikov et

al., 2013; Quigley et al., 2013; Jacoby et al., 2015; Hargitai, Levi, 2015; Ito et al., 2016; Rodríguez-Pascua et al., 2016; Onorato et al., 2016]. During years of research, it became apparent that the genesis of clastic dikes is multifarious [Owen, Moretti, 2011; Owen et al., 2011; Shanmugan, 2016, 2017] and, at first glance, to determine their origin seems to be complex.

Among the numerous publications, it is worth noting fundamental works of Jenkins [1925], Luper [1944], Fecht et al. [1999], Garetsky [1956], Kholodov [1978] and Braccini et al. [2008] dealing with the various aspects of clastic dikes. Their publications consider particularities of the dike distribution in different types of sediments and rocks, filling, morphology, possible sizes, origin, age, factors affecting their formation and methods of investigations. Specialized works devoted to sand blows from the epicentral areas of recent earthquakes appeared a while back. They provide information on criteria for seismic origin of clastic dikes resulting from liquefaction [Audemard, de Santis, 1991;

Obermeier, 1996, 1998; Obermeier et al., 2005; Lunina, Gladkov, 2016], open the possibilities of using these structures to locate the epicenter [*Green et al., 2005; Lunina et al., 2012*] and to estimate magnitude/macro-seismic intensity [*Lunina, Gladkov, 2015*], as well as show opportunities to date past earthquakes [*Tuttle, 2001; Porat et al., 2007*].

Nevertheless, the universal use of liquefaction structures to assess seismic hazards is still limited. This is because of problems of identification of seismic soft-deformation against the background of the structures of other genesis, as well as due to lack of depictive and quantitative data characterizing the blows of liquefied sediments from the epicentral areas of instrumental and historical events, which makes it difficult to apply the actualism for paleoseismological reconstructions. The search of dikes, which are not easy to reveal tens to hundreds of years after seismic shocks, is also a challenge. At the same time, liquefaction features in poorly exposed areas are often the only evidence of past disasters, so their findings and study are extremely important for predicting future earthquakes.

The goal of this work is briefly to systematize the available knowledge and to supplement them with new results of studying the clastic dikes to use them for seismic hazard assessments. The author of the paper below shows the diversity in origins of clastic dikes (i), revises geological and structural criteria of seismically induced injection dikes (ii), determines indicative criteria for liquefaction features on ground penetrating radar (GPR) images, as the GPR is most mobile and highly informative express method for scanning the subsurface (iii), and finally summarizes approaches for applying clastic dikes to earthquake study (iv).

2. TYPES AND ORIGINS OF CLASTIC DIKES

Depending on the fracture infilling directed upwards or downwards, clastic dikes are classified into two different groups [*Shrock, 1948; Garetzky, 1956; Montenat et al., 1991, 2007 Hargitai, Levi, 2015*]. The first one includes injection (intrusion, impact-fluidized) dikes formed by fluidized injection of clastic material into the host sedimentary layers and associated with overpressure buildup and hydraulic fracturing (Figs. 1, 2). It is relevant to recall here that liquefaction is the transformation of a granular material from a solid state into a liquefied state as a consequence of increased pore-water pressure and large loss of strength [*Youd, 1973*]. When a liquefied material rapidly penetrates through the overlying strata, the process is referred to as fluidization. The fluidization effects arise in poorly sorted clastic rocks covered by unconsolidated sedimentary layers with low permeability [*Moretti et al., 1999*]. The second group contains Neptunian (deposi-

tional) dikes formed by the introduction of material either under pressure or by the simple filling of pre-existing fissures from above (Figs. 3–5). As a rule, they are not associated with liquefaction, but in some cases, the infilling of small cracks occurs through the flowing of a liquefied material downwards. Subsequently, it can be seen associations of small injection and Neptunian dikes, 0.3–4.0 cm thick and 1–24 cm high, called micro-dikes [*Lunina et al., 2012*] or dikelets [*Levi et al., 2009*]. They are abundant in sands of various colors, which generally make up patterns of a “seismic cross section” (Fig. 6).

Among 21 triggering mechanisms that can initiate sediment failures in subaerial and submarine environments on Earth [*Shanmugam, 2016, 2017*], at least twelve main natural processes are responsible for forming clastic dikes and cylindrical bodies (Tables 1, 2): desiccation of soft deposits; extensional tectonics; flood; glacial loading; sudden deposition in underwater condition or in conditions of high humidity, including diagenesis in permafrost area; freeze-and-thaw action; tsunami; earthquake; inflow of fluid-generating clays in the region of high temperatures and overpressures and subsequent fracturing (mud volcanoes); storm waves; mass movement; and meteorite impact. Some triggers result in both types of dikes. With such diversity in the origins, at first glance, it is difficult to identify a seismically induced soft-sediment deformation. However, characteristic features allow excluding some nonseismic forms from paleoseismological analysis with a high degree of reliability. Thus, all clastic injections of non-seismic origin are geo-referenced to at least one of the geological objects (channel banks, glaciers, mud volcanoes, landslides, tsunamigenic beds and meteorite craters) and most of them are common in the subsurface layer to a depth of 1 m and have a cylindrical shape (Table 2). The configuration of seismically induced injection dikes implies a length many times greater than the width and a height varied from a few centimeters to the first ten of meters at a width less than 1 m. The dikes up to 15 cm wide occur the most frequently and those greater than 1 m are generally associated with lateral spreading through the horizontal extension forces [*Obermeier, 1996*]. Within the seismically active Dead Sea basin, injection dikes considered as an earthquake-induced structures are 5 mm – 18 m high and 1 mm – 0.18 m wide [*Levi et al., 2011*].

Neptunian dikes are often up to the first meters wide and sometimes have a laminated structure (Fig. 5) marking a stage-by-stage infilling of fractures (see Table 1). However, not all of them contain these characteristics and, therefore, for example, a permafrost wedge (see Fig. 4) could be mistaken for liquefaction features. On the other hand, Neptunian dikes also form in seismic shaking (see Fig. 3), but identification of their earthquake origin without other residual deformations

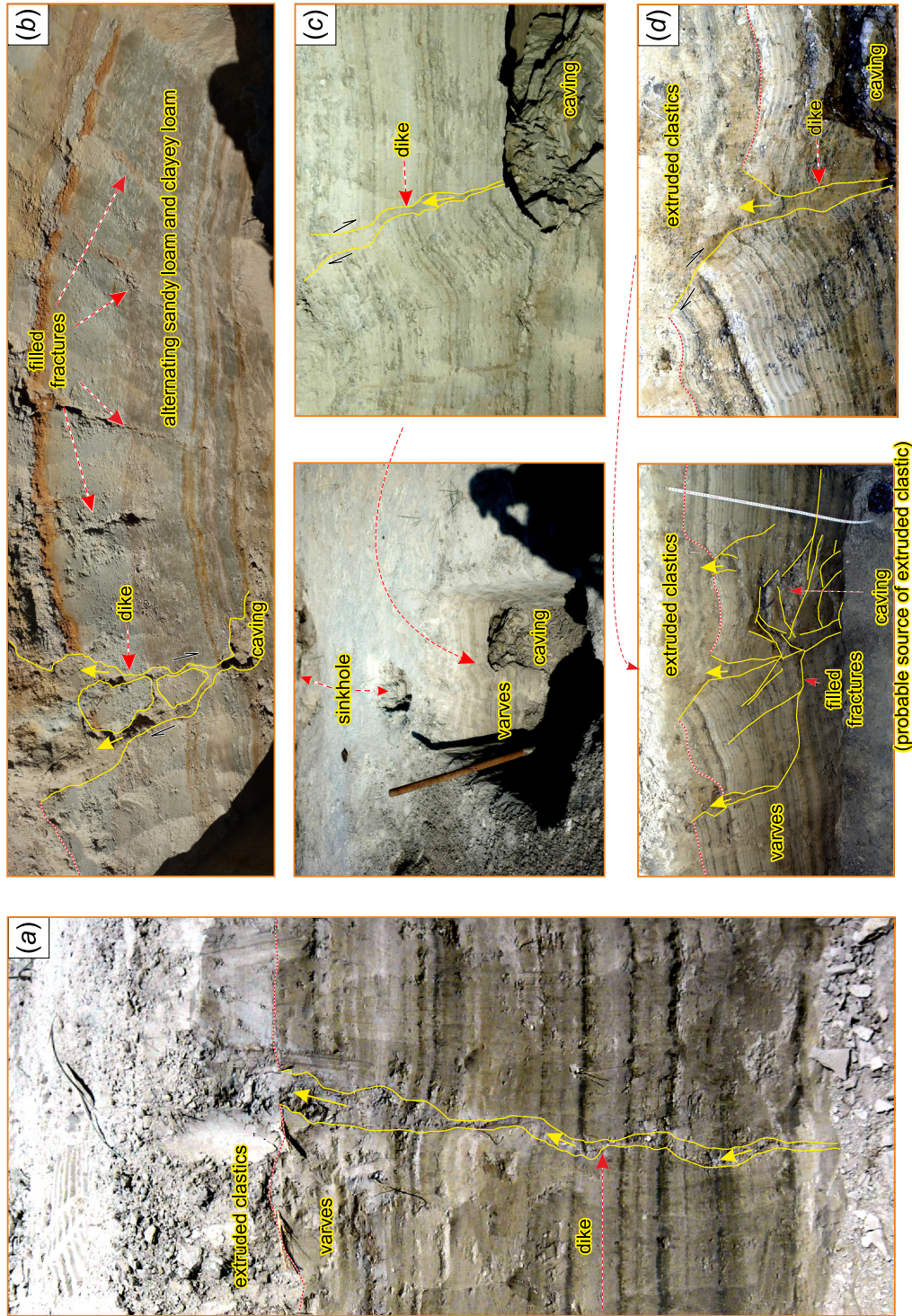


Fig. 1. Injection dikes formed by fluidized injection of thin clastic material into the host sedimentary layers during the $M_s=7.5$ Chuya earthquake of September 27, 2003 occurred in the southeastern part of the Gorny Altai (Russia): (a) – dike located at 49.98155°N and 88.15636°E, log height is 0.45 m; (b) – dike located at 49.94530°N and 88.12°E, log height is 1.31 m; (c) – dike located at 49.98139°N and 88.15637°E, log height is 1.1 m; (d) – dike located at 49.98154°N and 88.1563°E, log height is 1.1 m. The yellow arrows show an upward-directed movement of fluidized sediment during the seismic event. The dikes were revealed on the surface due to the presence of sinkholes.

Рис. 1. Инъекционные дайки, образованные внедрением тонкозернистого кластического материала в осадочные слои при Чуйском землетрясении 27 сентября 2003 г. ($M_s=7.5$), произошедшем в юго-восточной части Горного Алтая (Россия): (a) – дайка в точке наблюдения с координатами 49.98155°N и 88.15636°E, высота канавы 0.45 м; (b) – дайка в точке наблюдения с координатами 49.94530°N и 88.12°E, высота канавы 1.31 м; (c) – дайка в точке наблюдения с координатами 49.98139°N и 88.15637°E, высота канавы 1.1 м; (d) – дайка в точке наблюдения с координатами 49.98154°N и 88.1563°E, высота канавы 1.1 м. Желтые стрелки показывают направление движения флюидизированного осадка при сейсмических сотрясениях. Дайки выявлены благодаря воронкам на поверхности.

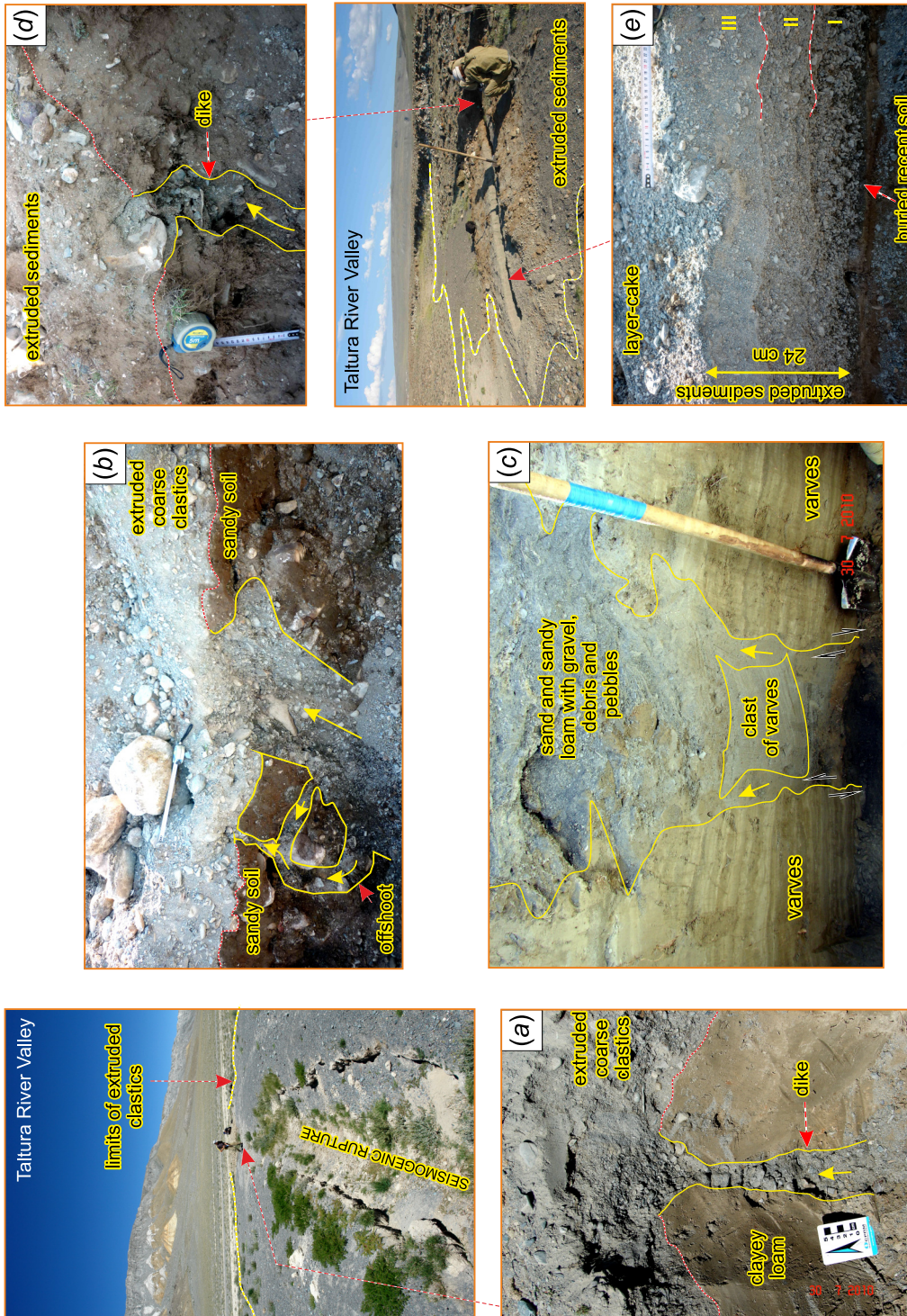


Fig. 2. Injection dikes formed by fluidized injection of coarse clastics into the host sedimentary layers during the $M_s=7.5$ Chuya earthquake of September 27, 2003 occurred in the southeastern part of the Gorny Altai (Russia): (a) – dike located at 49.93959°N and 88.11018°E, log height is 0.56 m; (b) – dike located at 49.97947°N and 88.14165°E, log height is 0.7 m; (c) – dike located at 49.97976°N and 88.14272°E, log height is 0.37 m; (d) – extruded sandy-gravel-pebble layers with a total thickness of 0.32 m. The yellow arrows show an upward-directed movement of fluidized sediment during the seismic event. The dikes were revealed on the surface due to the presence of sinkholes and extruded clastics on the surface.

Рис. 2. Инъекционные дайки, образованные внедрением грубообломочного кlastического материала в осадочные слои при Чуйском землетрясении 27 сентября 2003 г. ($M_s=7.5$), произошедшем в юго-восточной части Горного Алтая (Россия): (a) – дайка в точке наблюдения с координатами 49.93959°N и 88.11018°E, высота канавы 0.56 м; (b) – дайка в точке наблюдения с координатами 49.97947°N и 88.14165°E, высота канавы 0.7 м; (c) – дайка в точке наблюдения с координатами 49.97976°N и 88.14272°E, высота канавы 0.37 м; (d) – слой выброшенного песчано-гравийно-галечного материала общей мощностью 0.32 м. Желтые стрелки показывают направление движения флюидизированного осадка при сейсмических сотрясениях. Дайки выявлены, благодаря воронкам на поверхности.

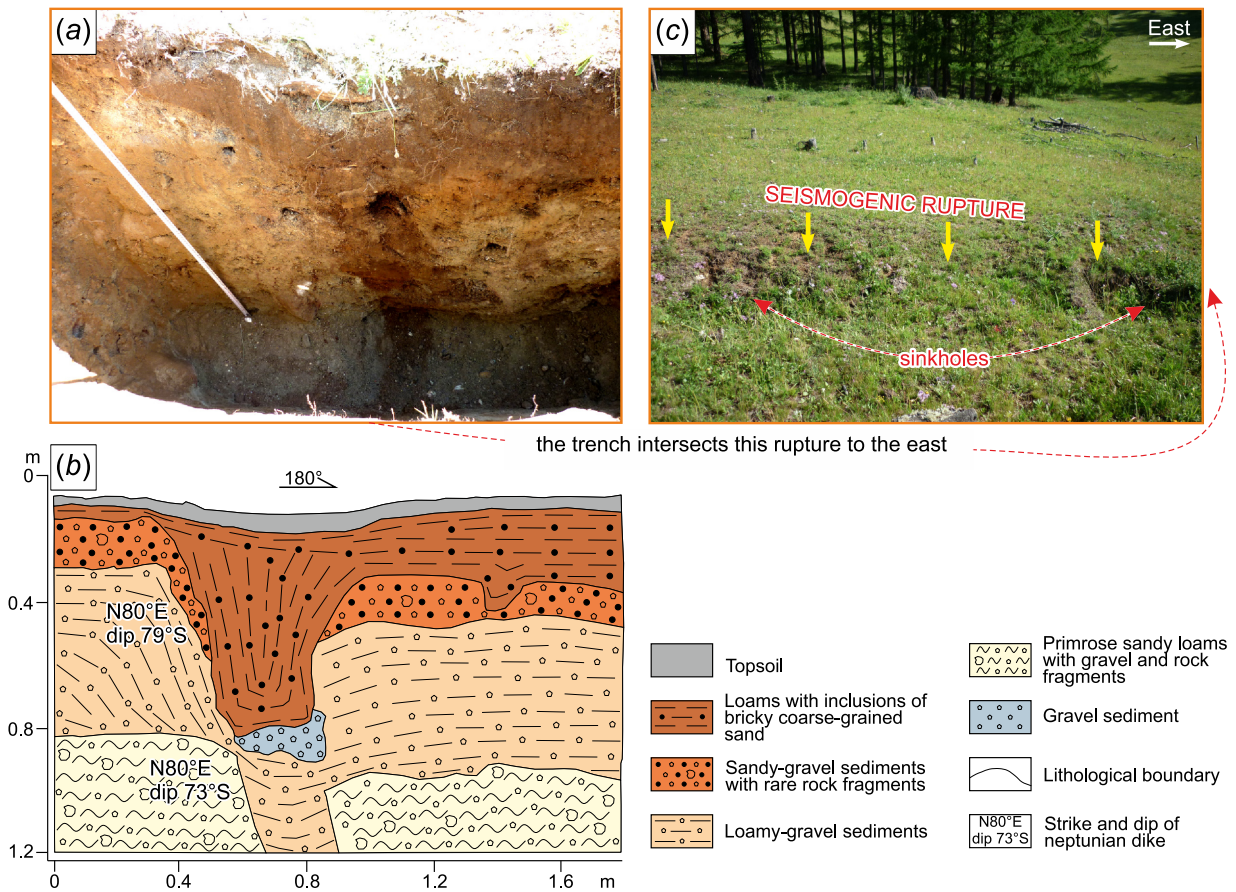


Fig. 3. Neptunian dike formed by filling of steep dipping seismogenic rupture from above (a) and interpreted cross section shown in a (site location: 51.68315°N and 100.98809°E) after [Lunina et al., 2015] (b); seismogenic rupture of the Mw=6.9 Mondy earthquake of April 4, 1950, occurred in southern East Siberia (Russia). The rupture has been uncovered by the trench shown in a (c).

Рис. 3. Нептуническая дайка, образованная путем заполнения сверху вниз крутопадающего сейсмогенного разрыва (a) и интерпретируемый разрез, показанный на рис. a (координаты точки наблюдения: 51.68315°N и 100.98809°E) по [Lunina et al., 2015] (b). Вскрытый канавой сейсмогенный разрыв Мондинского землетрясения с Mw=6.9, произошедшего на юге Восточной Сибири (Россия) 4 апреля 1950 г. (c).

is challenging. In this regard, for paleoseismic tasks it is better to rely on injection dikes and to take into account Neptunian ones only when additional evidence (surface ruptures, fractures with displacement of at least 0.1 m, structural analysis, relation to active faults etc.) is available. In addition, the injection dikes carry information about liquefaction susceptibility under certain cyclic loads determined by local characteristics of the oscillation amplitude and a duration of shaking that is especially important for engineers and designers. It has been illustrated that liquefaction occurs in the same place, repeatedly using the dikes to blow material [McCalpin, 2009].

Thus, considering the multifold natural processes, which could serve as triggers for the formation of clastic dikes, the study of seismic events should be based on relatively wide abundance of these structures and recognition of their earthquake genesis because of liquefaction and fluidization. Meanwhile, *Shanmugan*

[2016] and *Feng* [2017] believe that no unique criteria for separating seismic from nonseismic liquefaction exist. This opinion places in doubt using soft-sediment deformation for earthquake study. That is why the author of the present paper mainly focuses on the injection dikes, ignoring other types of soft-sediment deformations, and shows below that a consistent analysis of certain criteria allows proving their seismic origin.

3. INDICATIVE CRITERIA OF SEISMICALLY INDUCED INJECTION DIKES

3.1. GEOLOGICAL AND STRUCTURAL INDICATIVE CRITERIA OF SEISMICALLY INDUCED INJECTION DIKES

Most of the geological and structural criteria indicating seismic liquefaction refer to recognizing seismites

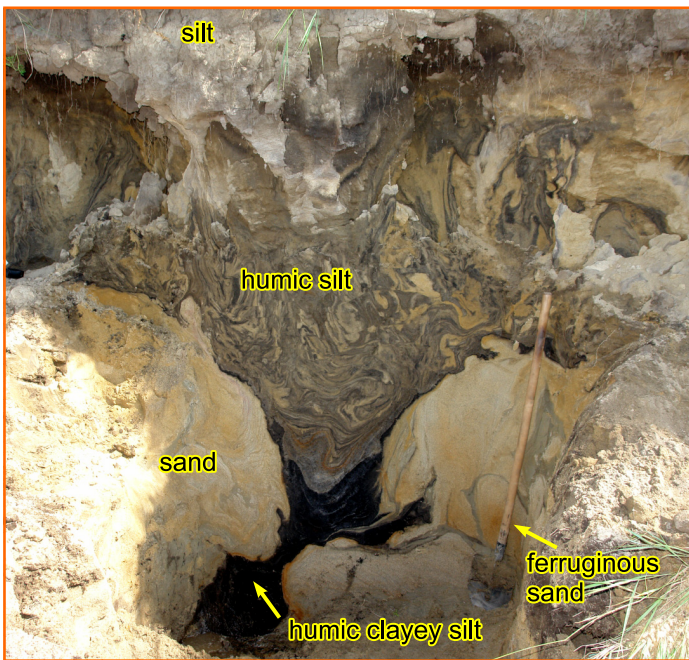


Fig. 4. Neptunian dike presented by a wedge filled with yellow and grey silt with a considerable amount of peaty and humic sediments, the Tunka basin of the Baikal rift zone (the photograph of A. Gladkov). The structure of the unconsolidated host deposits, the shape and size of the dike, as well as the physical-mechanical properties of the sediments point to a cryogenic origin of the shown deformation, as ice wedge pseudomorphs and cryoturbations [Alexeev et al., 2014].

Рис. 4. Нептуническая дайка клиновидной формы, выполненная желтым и серым пылеватым материалом со значительным количеством оторфованных и гумусированных отложений, Тункинская впадина Байкальской рифтовой зоны (фото А.С. Гладкова). Структура рыхлых вмещающих отложений, форма и размер дайки, а также физико-механические свойства осадков свидетельствуют о криогенном происхождении деформаций, отнесенных к псевдоморфозам клиновидной формы и криотурбациям [Alexeev et al., 2014].

[Sims, 1975; Anand, Jain, 1987; Seilacher, 1991; Rossetti, 1999; Greb, Dever, 2002; Wheeler, 2002; Montenat et al., 2007; Korzhenkov et al., 2014], which are stratigraphic units containing soft-sediment deformation produced by shaking [Seilacher, 1969; McCalpin, 2009; Van Loon, 2014]. The known features reflect the general conditions, under which the water-saturated unconsolidated deposits may become liquid. In addition, Obermeier [1996] proposed a feature of suddenly applied an upward-directed hydraulic force of short duration that

should appear in the sedimentary structure, as well described the characteristics of injection dikes from several seismic zones in the USA. Subsequently, based on the observations in the epicentral areas of instrumental and historical earthquakes, geological and structural criteria allowing directly on the outcrop to identify the seismic origin of injection dikes [Lunina, Gladkov, 2016] were developed. The author of the present paper revised all known features and analyzed specific descriptions of such structures to result in the

Fig. 5. Close-up of a touchet-type (laminated) Neptunian dike in the Touchet Beds of southeastern Washington (USA) resulted from catastrophic glacial outburst flooding (after [Spencer, Jaffee, 2012]). Cooley et al. [1996] suggest that the similar dikes were injected downward at or near the end of the most recent flood cycle and may have been the result of a combination of standing water in the valleys, seismic shock, and lateral spreading of poorly consolidated flood deposits.

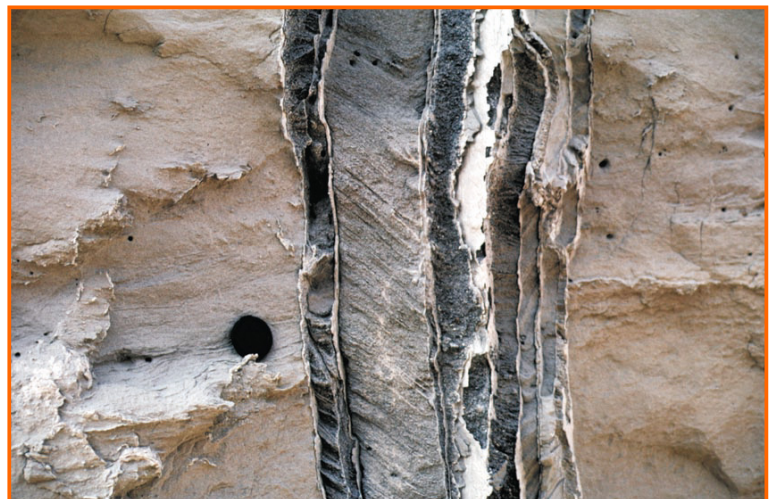


Рис. 5. Фрагмент расслоенной нептунической дайки из разреза «Touchet Beds» на юго-востоке штата Вашингтон (США), возникшей в результате внезапного катастрофического наводнения, связанного с таянием ледника (по материалам [Spencer, Jaffee, 2012]). Cooley et al. [1996] предполагают, что подобные дайки образованы путем заполнения трещин материалом сверху вниз в конце большинства современных паводковых циклов и могут быть результатом комбинации стоячей воды в долинах, сейсмических сотрясений и латерального распространения слабосцементированных наносов.

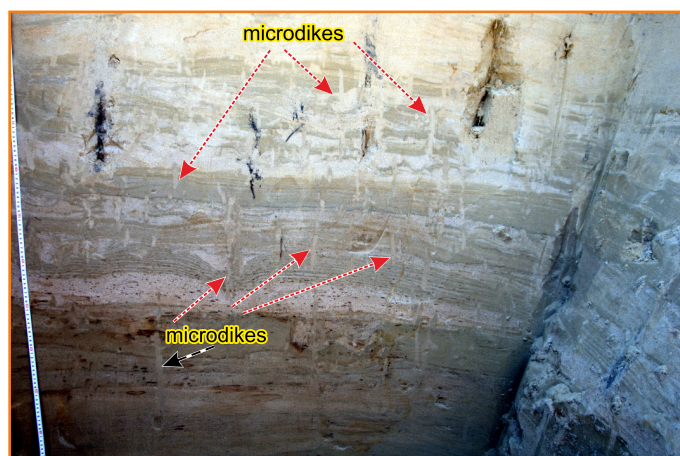


Fig. 6. Microdikes of whitish fine sand, up to 2 cm wide and 13 cm high, observed in a section of alternating loamy sands and sands (site location: 52.16056°N and 106.72708°E) at the epicenter area of the M~7.5 Tsagan earthquake occurred in the Proval Bay area of Lake Baikal on January 12, 1862 (after [Lunina et al., 2012]).

Рис. 6. Микродайки белесого тонкозернистого песка мощностью до 2 см в разрезе переслаивающихся супесей и песков (координаты точки наблюдения: 52.16056°N and 106.72708°E) в эпицентральной зоне Цаганского землетрясения с M~7.5, произошедшего 12 января 1862 г. в районе залива Провал на озере Байкал.

Table 1. Main triggers and formation mechanisms of Neptunian dikes and similar bodies

Таблица 1. Главные триггеры и механизмы формирования нептунических даек и подобных им тел

Triggers	Formation mechanisms	Some indicative features
Desiccation of unconsolidated deposits [Bump, 1951]	Gradual filling of fissures with overlying sediments	The laminated structure is typical of the dikes. The width of dikes is up to the first meters
Extensional tectonics [Moretti, Sabato, 2007]	Infilling of joints downward	
Flood [Cooley et al., 1996]	Slipping down wet sediments into fissures	The laminated structure is typical of the dikes. The width of the dikes is up to 3.5 m. The vertical stratification records a number of floods. Earthquakes could cause fractures during the floods
Glacial loading [Larsen, Mangerud, 1992; Passchier, 2000; Dionne, Shilts, 1974]	Formation of fractures under the glacier and infilling them (and earlier existing) downward by a plastic material or a mixture of water and sediments, including diamictites	Dikes consisting of clay to gravel can be of up to 2.5 m wide and 20 m long; both massive and laminated parallel to the walls. They typically dip down-glacier and strike perpendicular to the direction of ice movement, but may be vertical, at least in their upper portion. Process initiation requires that the base of the glacier is at the pressure-melting point
Sudden deposition in conditions of high humidity [Artyushkov, 1963a], including diagenesis in permafrost area [Kostyaev, 1969]	Convective instability or overloading (heavier layers slowly subside into lower, less dense sediments), cracking and infilling downward by overlying sediments	A smooth concordant folding of layers downward and confinedness of disturbances to bedding interface is characteristic of the situation. Infilling and host sediments at the bottom of structures undergo ductile crumpling and even intermix. The height of dike-shaped (wedge) structures is less than 1 m
Freeze-and-thaw action [Danilov, 1972; Ewertowski, 2009]	Melting of the wedge ice and formation of pseudomorphs, frost cracking and consequent infilling when thawing out	The dike-shaped structures (ice-wedges, pseudomorphs, frost cracks, veins) tapers downwards with a characteristic V-shaped morphology. Height could be up to 6 m, width – up to 3 m. A clay and loamy soil are filling, as a rule. Crack polygons develop on the surface
Tsunami [Le Roux et al., 2008]	The hyper-concentrated flow of water-saturated sand intrudes into underlying cohesive muds, plucking up large blocks of the latter and incorporating them into the flow	Both Neptunian and pseudo-injection dikes of several millimeters to 2 m wide and a few cms to more than 30 m long forms. They are usually massive but locally can be stratified parallel to the walls. As a whole, a high concentration of debris is typical of the sediments
Earthquake (many works)	Infilling of earthquake-induced ruptures resulting from wall caving, inflowing of liquefied sediment downward and/or later depositional	Dikes are typically massive; contain pieces of host sediments from the wall of rupture

Table 2. Main triggers and formation mechanisms of injection dikes and cylindrical bodies

Таблица 2. Главные триггеры и механизмы формирования инъекционных даек и цилиндрических тел

Triggers	Formation mechanisms	Some indicative features
Flood [<i>Li et al., 1996</i>]	Water seeping beneath levees and formation of sand boils	Flood-induced sand boils are limited to a narrow band along a river's levee; their conduits are most commonly tubular; depression of the ground surface is unusual; flood-induced sand boils are well sorted and fine; source bed is always near surface; materials removed from the walls surrounding a vent are rarely seen inside sand boils
Sudden deposition in underwater condition [<i>Artyushkov, 1963b; Moretti, Sabato, 2007</i>]	Convective instability or overloading, cracking and infilling upward by strong fluidized sediments	The structures have a small ratio of height and width and an elongated droplet shape. The host and intruding sediments undergo ductile deformation
Glacial loading [<i>Passchier, 2000; Cooley, 2015</i>]	Hydrofracturing, liquefaction and fluidization resulting from high pore-water pressures at the ice-bed interface when subglacial drainage is poor	Dikes form perpendicular to the direction of ice-flow, as a rule, near the edge of the glacier or the proglacial zone
Inflow of fluid-generating clays in the region of high temperatures and overpressures and subsequent fracturing [<i>Kholodov, 2002</i>]	Eruption of mud volcanoes	A source of the mud volcano is composed of clays (rarely sand), liquefied homogenized gas-water fluids (water, oil, gases of various composition), often with fragments of host sediments
Storm waves [<i>Alfaro et al., 2002</i>]	Liquefaction and fluidization as result of the cyclic effect of storm waves on unconsolidated sediments	Vertical cylindrical bodies like pipes are spatially associated with load structures and fluid escape structures. They locally reach up to 1 m in height and more than 2 m in width
Mass movement [<i>Iverson, 2015; Shanmugam, 2016</i>]	Liquefaction and fluidization resulting from high mobility of wet sediments, which are compressed as they destruct, giving rise to high groundwater pressures at the landslide base	Obviously, the structures should have a small penetration depth and a tubular shape. In most cases, heavy rainfall and earthquakes initiate mass movements
Tsunami [<i>Le Roux et al., 2008</i>]	Water-saturated sand flow intrudes into underlying cohesive muds, splitting large blocks and rotating them into the flow	Pseudo-dikes resulting from the block rotation in the mud flow form. Cylindrical bodies interpreted as upward fluid escape pipes, are possible. The rest characteristics see in Table 1
Meteorite impact [<i>Kring et al., 2004</i>]	Impact melt of sedimentary rocks	A clastic dolomite-dominated and hydrocarbon-charged dike crosscuts a limestone megablock beneath the melt-rich impactite sequence. The contact relationships are sharp and lack gradational disaggregation of the host. A number of limestone clasts occur throughout the dike matrix
Earthquake [<i>Obermeier, 1996, 1998; McCalpin, 2009</i>]	Liquefaction and fluidization resulting from cyclic loading during propagation of seismic waves	See descriptions of features in sections 2 and 3.2 of the present paper

formulation of general and individual criteria that are valid for the seimogenic genesis of injection dikes.

General indicative criteria of seismically induced injection dikes are following:

1. Soft-sediment deformation is located within 200 km from an active fault (maximum distance, at which liquefaction effects can be manifested according to world data [*Ambraseys, 1988*]).

2. Suitable sediment composition – poorly consolidated metastable sands with low cohesion, loamy sand, varves, sand-gravel-pebble sediments. Capable of fluidization unconsolidated and poorly consolidated sediments are covered by layer of lower permeability.

3. A flat area, which excludes gravity flow.

4. Ruling out the possibility of an origin from artesian water.

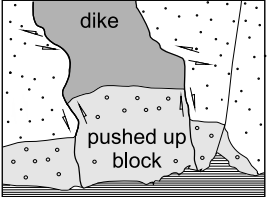
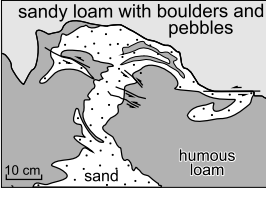
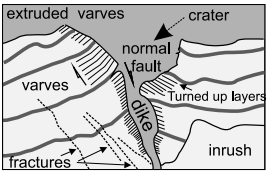
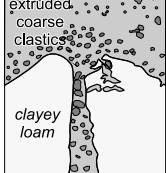
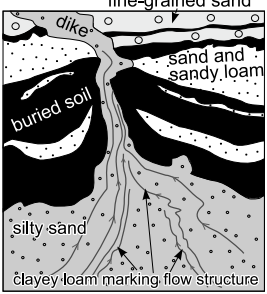
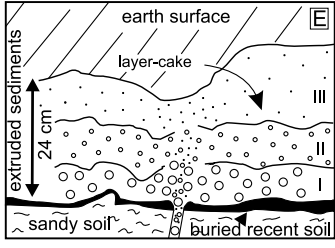
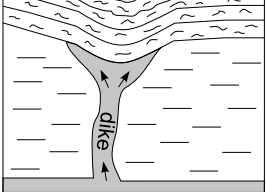
#	Criterion	Schematic view of resulting seismogenic features	Criterion	Schematic view of resulting seismogenic features
1	Pushed up sedimentary blocks within the dike body		8	
2	Regular distorted contacts of dike with host sediments, reflecting cyclic loading during propagation of seismic waves		9	
3	Turned up layers of host deposits on contacts with a dike		10	
4	Displacement along dike contacts usually in the form of a normal fault caused by subsidence that compensates for the removed sediment			
5	Filled crater			
6	Flow structures project upward from liquefied layer into the bottom of the dike		11	
7	Large amount of downwarping of the cap toward the dike			

Fig. 7. Individual indicative criteria of seismically induced injection dikes for study in sectional view.

Рис. 7. Индивидуальные критерии идентификации сейсмогенных инъекционных даек в разрезе.

5. Absence of nonseismic landsliding, channel banks and traces of ice shelf in the vicinity.

6. Absence of impact craters and mud volcanoes in the vicinity.

7. Avoiding tsunamites and tempestites in the section, as well as localities of sudden deposition.

8. Similarity between investigated dikes and historically documented dikes of the earthquake induced liquefaction processes, in a similar physical setting.

9. The dike locations are identified on the surface by sinkholes, whose long axes coincide with the strike of the dikes in most cases (the criterion is valid for recent earthquakes).

10. The smaller dikes are closer to each other than the larger ones [Obermeier, 1996].

11. Dikes occur at multiple places, preferably at least within a few kilometers of one another, in similar geologic and ground water settings [Obermeier, 1996; McCalpin, 2009], and satisfy magnitude/distance relations for liquefaction from earthquakes.

12. The evidence for age of the dikes supports the interpretation that they formed in one or more discrete, short episodes that individually affected a large area and that the episodes were separated by relatively long time periods during which no such features formed [Obermeier, 1996; McCalpin, 2009].

Individual criteria of seismically induced injection dikes in sectional view are following:

1. Pushed up sedimentary blocks within the dike body (see Fig. 2, c, Fig. 7). The rise of the layer was apparently due to the pressure of water flow that penetrates the deposits through the fractures and infiltrates host sediments, partly inplacing them mostly along walls of the structure. This feature is relevant even when dike morphed by cryogenic processes (Fig. 8).

2. Regular distorted contacts of dike with host sediments (see Fig. 2, c-d, Fig. 7), reflecting cyclic loading during propagation of seismic waves [Obermeier et al., 2005]. This feature usually occurs with criterion 1.

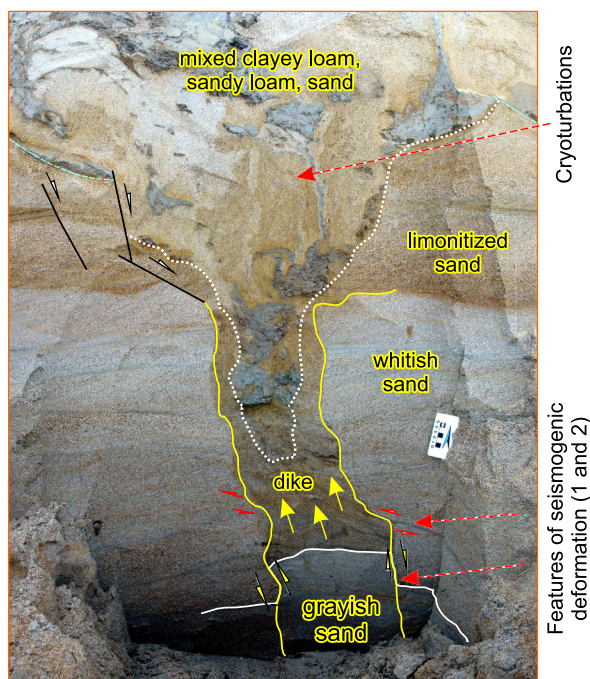


Fig. 8. Ice wedge pseudomorphs superimposed on seismogenic sand dike on the right bank of the Irkut river near the Zhemchug settlement (Holocene sediments in the Tunka basin of the Baikal rift zone, site is located at 51.71429°N and 102.43690°E).

Рис. 8. Псевдоморфозы клиновидной формы, наложенные на сейсмогенную песчаную дайку в разрезе правого берега р. Иркут вблизи пос. Жемчуг (голоценовые отложения Тункинской впадины Байкальской рифтовой зоны, координаты точки наблюдения: 51.71429°N, 102.43690°E).

3. Turned up layers of host deposits on contacts with a dike (see Fig. 1, *c-d*, Figs. 7, 9). The feature is typical of laminated sedimentary rocks. It differs from ice-wedge pseudomorphs and relict frost cracks, in which all host layers in contact with the inner zone of fill derived from above and from sides, are lowered [Ewertowski, 2009] in the direction of water movement when thawing the soil near the surface.

4. Displacement along dike contacts usually in the form of a normal fault caused by tectonic movements or subsidence that compensates for the removed sediment (see Fig. 1, *c-d*, Fig. 7). Like seismogenic features 1 and 2, this helps the recognition of an earthquake-triggered dike affected by cryogenic processes

5. Existence of craterlet filled like a colluvial wedge (see Figs. 1, *b, d*, Fig. 7). Exogenous processes often truncate the craterlets.

6. Flow structures project upward from the liquefied layer into the bottom of the dike and testify upward-directed hydraulic force [Obermeier, 1996] (Figs. 7, 9).

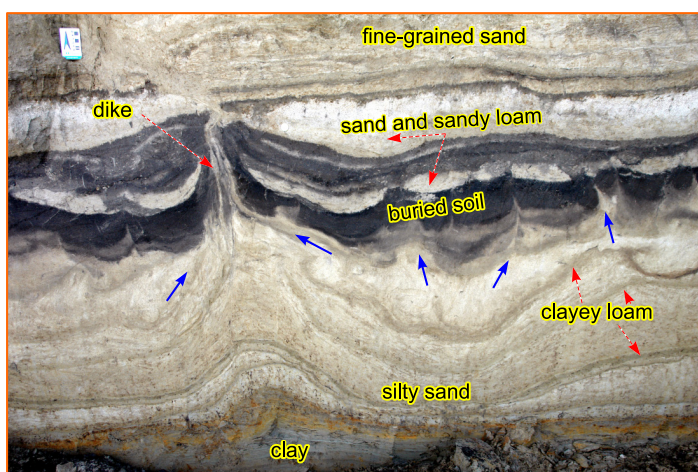
7. A large amount of downwarping of the cap toward the dike (more than 0.5 m) (see Fig. 7). It tends to be most pronounced where a large amount of sediments has vented to the surface [Obermeier, 1996]. Unlike criterion 4, this downwarping can be either one or both sides, and overlying strata are cracked without a displacement.

8. A dike structure like a diapir subject to fulfilment of next criterion 9 (Fig. 7). Such a structure is characteristic of dike infilled by fluidized material, which was injected vertically and then between layers, not reaching the surface.

9. Filling of an injection dike with coarser material than the host sediments (see Fig. 2). This separates

Fig. 9. Flow structures projecting upward from the source zones into the dike and indicative of an upward-directed hydraulic force (Holocene sediments on the left bank of the Irkut river near the Guzhiry settlement in the Guzhiry fault zone, the Tunka basin of the Baikal rift zone, site is located at 51.78502°N and 102.89063°E).

Рис. 9. Структуры течения, указывающие на проникновение осадка из зоны разжижения в дайку под действием направленной вверх гидравлической силы (голоценовые отложения в левом борту р. Иркут вблизи села Гужиры в зоне Гужирского разлома, Тункинская впадина Байкальской рифтовой зоны, координаты точки наблюдения: 51.78502°N и 102.89063°E).



earthquake-triggered liquefaction deformation from loam diapirs originating from cryostatic pressure and gravitational loading of sediments, as well as from ice-wedge and frost cracks filled with more fine-grained deposits in comparative with the host sediments. It also allows the derivation of seismogenic dike after the influence of the cryogenic processes on seismically deformed sediments.

10. A sediment layer extruded on the surface or between the strata, similar in composition to the dike (see Figs. 2, 7). The layer should be absent in adjacent correlated sections.

11. In the extruded sandy-gravel-pebble bed and inside the dike, the rock fragments show normal grading from large to small clasts (see Fig. 2, *d–e*, 7). This is because the reduction of seismic vibrations during the earthquake decreases the size of ejected sedimentary debris on the surface [Lunina, Gladkov, 2016]. It is possible that some large blows have more than one vertical sequence of the vented sediment [Obermeier, 1996; McCalpin, 2009]. A lack of intervening pedological development between sequences will show more than one discrete episode of injecting, closely spaced in time [Saucier, 1989]. In contrast, in the case of observed soil evolution, it is possible to define a recurrence interval of earthquakes.

12. Fractures occur along with dikes in the sequences (see Fig. 1, *b*) and dominant directions of the dikes are close to the orientation of major and/or secondary active faults or these fractures (see Figs. 5, 13 in [Lunina, Gladkov, 2016]).

Diagnosing the several individual criteria allows to separate injection dikes clearly from Neptunian ones right on an outcrop and to exclude from consideration triggers that are specific for latter (see Table 1). It is also possible to distinguish structures resulting from fluidization and superimposed cryogenic formations when they are observed in a sectional view together (see Fig. 8). This is because earthquake deformation may result in changing conditions of heat and mass exchange as well as the physical and mechanical parameters of the ground surface, in particular its strength properties, porosity, density, and moisture. As a result, there is degradation of permafrost, increasing the depth of the seasonal freeze/thaw of soils and their migration in the deformed sediments with formation of cryoturbations and bending of layers, and sinkholes and subsidences on the surface.

Sharing the general and individual criteria completely excludes nonseismic triggers that could cause liquefaction and fluidization. If only tabular dikes are observed, for instance, flood, storm waves, tsunami and mass movements may not be regarded as a trigger to form these structures because of tubular bodies (Table 2), as a rule, are developed during the listed hazards. In most cases, they are less than 1 m high, but

there are exception for tsunami origin [Le Roux *et al.*, 2008]. In contrast, large dikes whose heights exceed a meter or so and whose widths exceed several centimeters will support the seismic origin associated with fluidization from liquefaction [Obermeier, 1996].

Some of the indicative criteria of seismically induced injection dikes should be strictly adhered (general criteria 1, 2, 6, and 7, individual criterion 9). Others may appear or may be not manifested (general criterion 9, individual criteria 1, 2, 3, 6, 8, 11, and partially 12), be obscured by superimposed exogenous processes (individual criteria 5, 4, and 7) or remain unknown (general criteria 8, 10, 11 and 12, individual criteria 6, 10, and partially 12) a case-by-case basis. This is because the forms and types of seismogenic soft-sediment deformations depend on the lithology and structure of the sediments [Moretti *et al.*, 1999], as well as on depth of the water table [Obermeier *et al.*, 2005] and if the fluidized mass was extruded on the surface or between layers. Furthermore, the higher peak ground accelerations are the greater the likelihood of forming injection dikes and the wider areas covered by liquefaction, other things being equal. It should also be assumed that given the widespread development of injection dikes of more than 1 m high and compliance with most indicative criteria of their seismic origin (including necessarily the general criterion 11 and individual criterion 12), general criteria 3 and 5 can be ignored. These assumptions are possible because seismic shocks affect different landscapes and many nonseismic triggers cause a local spreading of small-sized structures of specific forms. The fact that soil liquefaction begins in earthquakes with $M \geq 5.2–5.5$ [Ambraseys, 1988; Lunina *et al.*, 2014], which corresponds to the MSK-64 macroseismic intensity of at least 6, proves it. It is unlikely that such shaking can be caused by a landslide or a movement of a glacier within a radius of even a few kilometers. In addition, during a seismic event, artesian waters can outrush through cracks and washed up fluidized material to the surface, which also implies a possible ignoring of the general criterion 4. Thus, each case must be carefully considered, taking into account the above recommendations, as well as the geological, structural and geomorphologic environments.

3.2. INDICATIVE CRITERIA OF INJECTION DIKES AND OTHER LIQUEFACTION FEATURES ON GPR IMAGES

While a final solution about the seismogenic origin of the injection dikes must be accepted, based on geological and structural indicative criteria, preliminarily these structures and other liquefaction features might be found on GPR images. Most of GPR works conclude that sand blows on radargrams are shown as stratigraphic disruptions of the radar events and disturbance of the GPR facie [Liu, Li, 2001; Al-Shukri *et al.*, 2006; Nobes *et al.*, 2013; Baradello, Accaino, 2016]. Charac-

teristic anomalies, the shape of which is like a funnel or a pipe with disordered and stronger reflection are additional indicators of liquefaction on GPR images [Hsu *et al.*, 2005; Lunina, Gladkov, 2016].

In the summer of 2013 and 2015, we carried out systematic GPR studies on the southeastern coast of Lake Baikal in the epicentral area of the devastating January 12, 1862 Tsagan earthquake ($M \sim 7.5$) known for its abundant manifestations of liquefaction and fluidization [Lunina *et al.*, 2012]. We used the Logis-Geotech OKO-2 radar, which consists of a control processing unit, an odometer DP-32, a transportation handle, power supply unit (BP 9/12), charge (ZU-9), connection cables, and a AB-250 M screened antenna with 250 MHz, all made in Russia. The AB-250M antenna is a monoblock integrating receiving and transmitting parts in one enclosure. Its specifications correspond to 8 m maximum penetration depth and 0.25 m vertical resolution capability. Sixteen GPR profiles 42–160 m long were surveyed on five testing grounds across the strike of the Delta coseismic fault scarp between Kudara and Oimur Villages. Shallow drilling and trenching in the selected sites showed a homogeneous section throughout the study area, which is represented by loamy sand, sand of various grain colors and sizes, sandy loam and gray water-saturated sand. When processing and interpreting the GPR profiles, we identified numerous anomalies that were associated with liquefaction features (Fig. 10), based on observations in the trenches exposing some of them. Relatively high values of unipolar positive echoes on the trace of GPR signal mark all anomalies.

In accordance with form, the anomalies were grouped into four types. The most common pipe-shaped vertical anomalies 0.4–0.7 m wide correspond to individual injection dikes (Fig. 10, *a*) and belong to the first category. Some pipe-shaped vertical anomalies are visible on parallel GPR profiles that is the best criterion of sand blow in a sedimentary section (Fig. 10, *b*). The position of the GPR profiles provides a measure of the dike strike. Anomalies of the second type take a platy shape in the section and represent region of a width several times greater than their height (Fig. 10, *c*). Anomalies of the third type are isometric or irregular (Fig. 10, *d*). Wide zones up to 3 m thick combining a pipe-shaped form in the lower part and isometric in the upper part refer to anomalies of the fourth type (Fig. 10, *e*). Digging up one of them, we have discovered at depths of 1.40–2.68 m a field of intensive manifestation of microdikes of whitish sand in fine-grained limonitized sand. These microdikes stand out from the background of chaotic association of structures resulting from liquefaction and fluidization. The examination of anomalies suggests that anomalies of second and third types fit regions, wherein process of fluidization are less developed. In general, judging from geology of sections, fine-medium- and fi-

ne-grained sands covered by silty sands and loamy sand were liquefied in all cases.

The anomalies of first and forth types are the most perspective for further geological and structural exploring. Based on them, indicative criteria of injection dikes on GPR data emerge: a pipe-shaped anomaly or a composite anomaly combining a tubular form in the lower part with an isometric – in the upper (*i*); relatively high values of unipolar positive echoes on the trace of GPR signal (*ii*); an occurrence of the same anomaly on adjacent parallel profiles located the first tens of meters apart (*iii*). All three signs should be expressed on radargrams to reveal and preliminary to identify earthquake origin of an injection dike. Additionally, stratigraphic disruptions of the radar events on the background of their continuous horizontal position should be considered as the fourth independent criterion (*iv*) established earlier [Liu, Li, 2001]. At the same time, it cannot be excluded that the same forms of anomalies will be associated with other irregularities in the sedimentary section so it is important to dug at least several key objects for confirming the existence of dike and its seismic origin.

4. CONSTRAINING THE AGE OF PALEOEARTHQUAKE BASED ON CLASTIC DIKES

When confirming a seismic origin of dikes, one can begin to constrain the age of paleoevents. According to the general principals of their dating based on a coseismic deformation, the earthquake age is bracketed by the time interval between ages of the youngest faulted bed [lower limit] and the oldest unfaulted bed overlying sedimentary facies genetically related to this earthquakes (upper limit) [McCalpin, 2009]. In the study of clastic dikes, it is desirable to estimate the ages of the host and overlapping strata and/or the age of the material infilling the fracture. However, this condition cannot always be fully because of the lack of right material to a certain dating method. In this case, a definition of the dike type facilitates paleoearthquake dating and avoids any misunderstanding. Indeed, the infilling of Neptunian dike can be attributed to coseismic sedimentation by analogy with a colluvial wedge and based only on clasts in this dike to establish the approximate date of the related faulting [Lunina *et al.*, 2015]. This is because the filling of the dikes, like the formation of the colluvial facies, takes place in short time interval [McCalpin, 2009]. In comparison with the buried soil or other kinds of sediments, artifacts or tree trunks inside the dike will be the strongest predictor of a calendar age.

If injection dikes is identified in the section and the boundary between the vented material and the underlying soil horizon is clearly visible, as we observed in the 2003 Chuya earthquake in the Gorny Altai (see

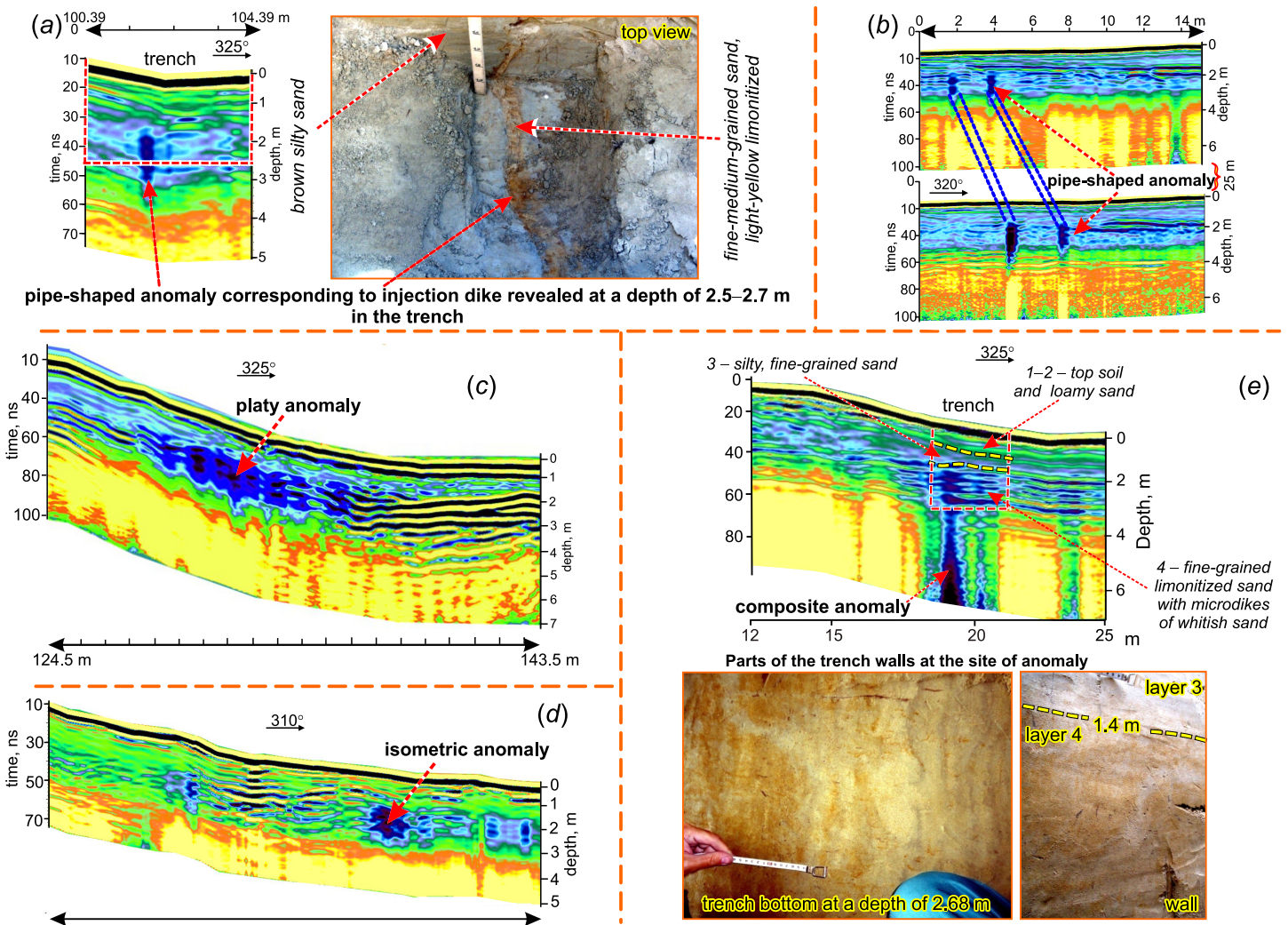


Fig. 10. Anomalies of various shapes corresponding to liquefaction features on GPR images acquired by using Logis-Geotech OKO-2 radar with AB-250 MHz antenna in the epicentral area of the 1862 M~7.5 Tsagan earthquake affected the eastern shore of Lake Baikal: (a-b) – pipe-shaped; (c) – platy; (d) – isometric; (e) – composite anomaly combined the pipe-shaped and isometric configurations. The Tsagan earthquake is well-known for widespread sand blows in the Delta fault zone, which extends from the Selenga River delta to the north-east along the southeastern shore of Lake Baikal. The photographs in Figs. (a) and (e) show fragments of sections at the sites of anomalies.

Рис. 10. Аномалии различной формы, ассоциируемые с признаками разжижения на радарограммах, полученных с использованием георадара ОКО-2 и антенны АБ-250М в эпицентральной зоне Цаганского землетрясения 1862 г. с М~7.5 на восточном побережье озера Байкал: (a-b) – трубообразные; (c) – плитообразная; (d) – изометрическая; (e) – сочетание трубообразной формы в нижней части с изометричной – в верхней. Цаганское землетрясение хорошо известно выбросами разжиженного песка в зоне Дельтового разлома, который простирается от дельты р. Селенги на северо-восток вдоль юго-восточного побережья озера Байкал. Фото на рис. (a) и (e) показывают фрагменты разрезов в местах аномалий.

Fig. 2, e) and other researchers noted [Castilla, Aude-mard, 2007], then it is enough to know the age of the buried humus layer in its roof to date seismic event. In other cases, general principles should be followed for these purposes, although a researcher is aware that not all clastic intrusions, just like ruptures [Bonilla, Lien-kaemper, 1991], can reach the surface. Such injections often pinch together upward or spread out between the layers in the form of sills, so they are not hard to recognize. Examples of how liquefaction features to use

for constraining the age and other parameters of paleo-earthquakes are demonstrated in the following works [McNulty, Obermeier, 1997; Cox et al., 2007].

5. LOCALIZATION OF A PRE-INSTRUMENTAL EARTHQUAKE EPICENTER

With a sufficient number of observation sites and justification of the dike coevality, they may be used to

localize the epicenter of the pre-instrumental earthquake. Hence, *Green et al. [2005]* treated the widths of dikes and by simple interpolation plotted a map of iso-lines to perform that task (see fig. 8 in fore-quoted work). Based on these results, the author of the present paper have showed a possibility for reconstruction of the epicenter of the 1862, $M \sim 7.5$, Tsagan earthquake through the analysis of various parameters of the clastic dikes and associated secondary coseismic deformations, taking into account the dip of the causative fault and the average origin depth of earthquakes in the Baikal rift zone [*Lunina et al., 2012*].

The core of this tool is that, in the first stage, a researcher plots graphs of variations of parameters of observed structures (Fig. 11, *stage I*). It is possible to apply available characteristics but the more of them the more reliable the result. We used the following attributes: maximum displacements D_{max} for the intra-layered reverse and normal faults; ratio of the number of faults with the displacements to the length of cleaning (N_s/L); thickness of the tectonic zone (m_{tz}); number of fractures per square meter (N); the mean width (w_{cd}) and height (h_{cd}) of the clastic dikes; the ratio of the number of clastic dikes to the length of cleaning (N_{cd}/L); the mean index of intensity of clastic dyke manifestation (I_{cd}); the mean width (w_{md}) and height (h_{md}) of microdikes; the ratio of the number of microdikes to the length of cleaning (N_{md}/L); and the mean index of intensity of microdike manifestation (I_{md}). We introduced parameters I_{cd} and I_{md} to take into account the set of all characteristics measured. The mean index of the intensity of manifestation of individual clastic dikes in the cleaning (I_{cd}) are calculated from the relation

$$I_{cd} = N_{cd} \times w_{cd} \times h_{cd} \times 10000 / H \times L,$$

where N_{cd} is the number of dikes, w_{cd} is the mean width (m), h_{cd} is the mean visible height of dikes in the section (m), H is the height of cleaning (m), and L is the length of cleaning (m). The relation for determining the mean index of intensity of microdike manifestation is similar

$$I_{md} = d \times N_{md} \times w_{md} \times h_{md} \times 10000 / H \times L,$$

where d is the coefficient reflecting the ratio of the minimum thickness of the sedimentary rhythm to the maximum thickness. The rhythm is a pair of two alternating sedimentary layers with different composition and properties, within which the microdikes are observed.

In the second stage, the data on the distribution of coseismic deformations in the soft sediments are synthesized by means of the procedure of calculating the sum of all significant peaks (on the graphs) for all analyzed parameters at each sites (SUM_{spp} , an abbreviation for the sum of significant parameter peaks) (Fig. 11,

stage II). The values, which are greater than the arithmetic mean for both profiles, are considered the peaks. Based on the values of SUM_{spp} , contour lines on the plan are plotted and maximum value of SUM_{spp} corresponding to the largest shaking are bounded (Fig. 11, *stage II and III*).

In the third stage, a more detailed location of the epicenter is based on the correlation with the active fault. At an average dip angle of the causative Delta fault of 60° [*Lunina et al., 2012*] and at an average depth of the earthquake source in the Baikal Rift Zone of 15 km [*Gileva et al., 2000*], hypocenter projected normally on the day-time surface would be located at a distance of 8.7 km from the main fault. Then, we put on our plan the segment equal to the calculated distance from the Delta Fault along their dip azimuth from the central part of the region with the maximum intensity of coseismic deformations and got the sought epicenter of the Tzagan earthquake (Fig. 11, *stage III*).

Thus, analysis of one parameter of clastic dikes would be enhanced by study case of several characteristics of soft-sediment deformations in combination with other data, including the faults and the current seismicity of the region under consideration.

6. ESTIMATION OF THE LOWER-BOUND MAGNITUDE/INTENSITY OF PRE-INSTRUMENTAL EARTHQUAKES

The opportunities of using seismically induced clastic dikes in a seismic hazard analysis include also an estimation of the energy of an earthquake. To measure it based on liquefaction features, empirical relationships between the magnitude and the epicentral or fault distance are applied [*Kuribayashi, Tatsuoka, 1975; Youd, Perkins, 1978; Liu, Xie, 1984; Ambraseys, 1988; Papadopoulos, Lefkopoulos, 1993; Wakamatsu, 1993; Galli, 2000; Papathanassiou et al., 2005; Lunina et al., 2014*]. These relationships are effective in the case of a known location of the seismogenic source that is responsible for liquefaction. Castilla and Audemard [2007] suggested the additional use of the curve of the sand-blow diameter versus the epicentral distance. This approach promoted a potential of assessing the magnitude on basis of liquefaction features but eroding the sand-blow cones before their burial restricts using the corresponding relations.

At the same time, venting pipe always remains in a section, which allows to establish the lower-bound magnitude of the paleoseismic event and the local macroseismic intensity by applying the bounding relationships between the earthquake parameters and geometries of clastic dikes produced by instrumental earthquakes. The author of the present work and her colleague first introduced such equations and the

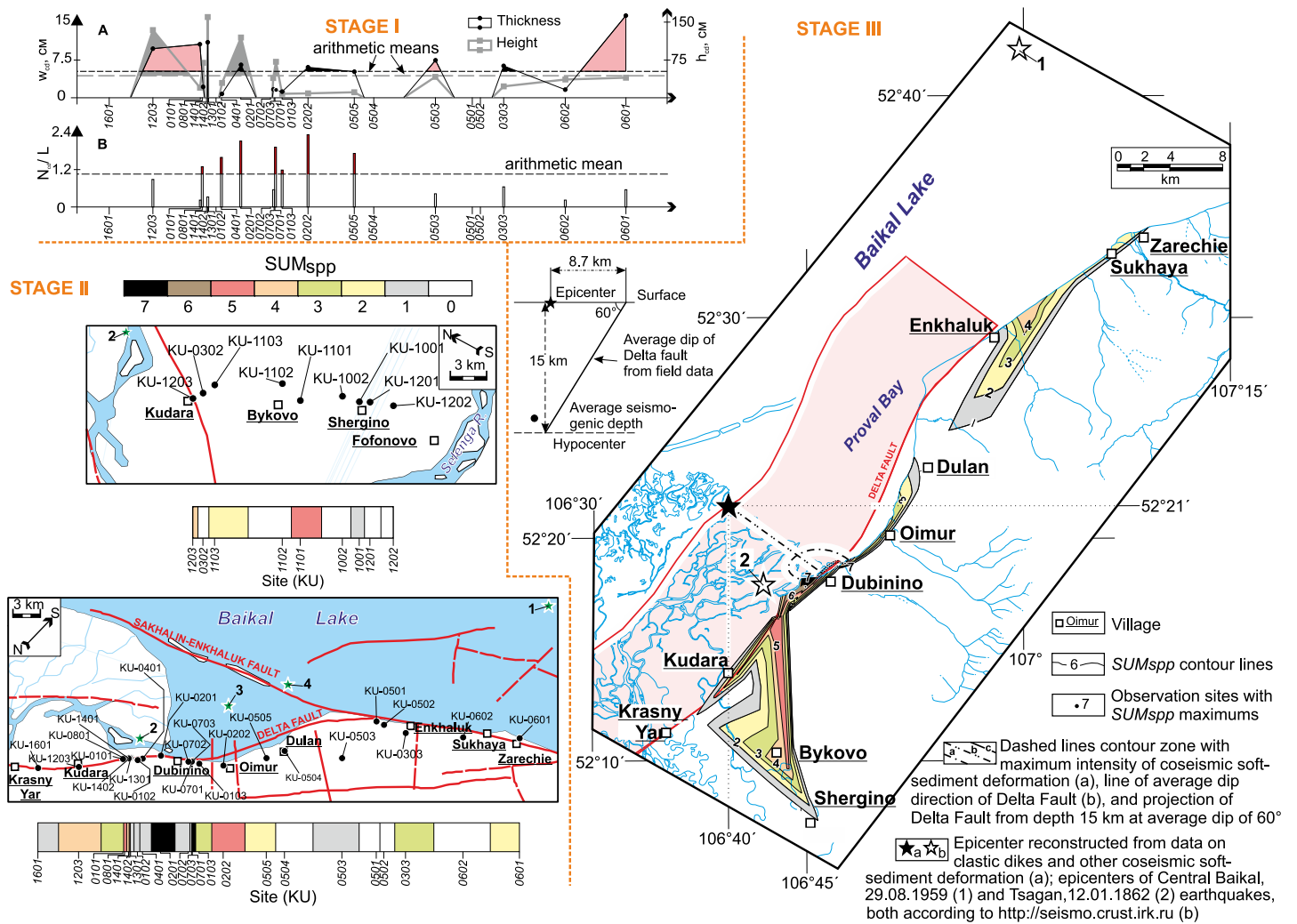


Fig. 11. Example of location of earthquake epicenter (for Tsagan event of 1862 occurred in Baikal region) from parameters of clastic dikes and other coseismic soft-sediment deformation, taking into account dip of causative fault and average seismogenic depth: STAGE I – graph plotting showing distribution of parameters of coseismic soft-sediment deformation along profile Krasny Yar–Zarechie (in this case: average thickness (w_{cd} , cm) and height (h_{cd} , cm) of clastic dikes (A), as well as N_{cd}/L ratio (B), where N_{cd} is number of clastic dikes and L is length of a cut). All graphs have been published in [Lunina et al., 2012]; STAGE II – analysis of distribution of $SUMspp$ (the sum of significant parameter peaks) along the profiles for the parameters included in analysis, and respective scales; STAGE III – reconstruction of epicenter from maximum of $SUMspp$, dip of the Delta Fault plane and average seismogenic depth in the Baikal rift zone.

Рис. 11. Пример локализации эпицентра землетрясения (для Цаганского события 1862 г. в Байкальском регионе) по параметрам кластических даек и другим косейсмическим деформациям в рыхлых осадках с учетом угла падения плоскости сейсмогенерирующего разлома и средней глубины землетрясений: STAGE I (стадия I) – построение графиков распределения параметров косейсмических деформаций вдоль профиля «с. Красный Яр – с. Заречье» (в данном случае средней мощности (w_{cd} , см) и высоты (h_{cd} , см) кластических даек (A), а также отношения N_{cd}/L (B), где N_{cd} – количество кластических даек, L – длина разреза). Все графики опубликованы в [Lunina et al., 2012]; STAGE II (стадия II) – анализ распределения $SUMspp$ (суммы значимых пиков параметров косейсмических деформаций) для параметров, включенных в анализ и соответствующие шкалы; STAGE III (стадия III) – реконструкция местоположения эпицентра на основе максимального значения $SUMspp$, угла падения Дельтового разлома и средней глубины землетрясений в Байкальской рифтовой зоне.

underlying worldwide data [Lunina, Gladkov, 2015]. Maximum width (w_{cd}), visible maximum height (h_{cd}) and intensity index of clastic dikes (I_{cd}) were correlated with the surface-wave magnitude (M_s) and local macroseismic intensity (I_L) corresponding to the MSK-64 macroseismic intensity scale. Here it would be ap-

propriate to discuss the pros and cons in applying the bounding relationships (Fig. 12, a–c) that are valid both for Neptunian and injection dikes of earthquake origin.

Because only the end points are used to generate the curves (Fig. 12, a–c), the determination coefficients

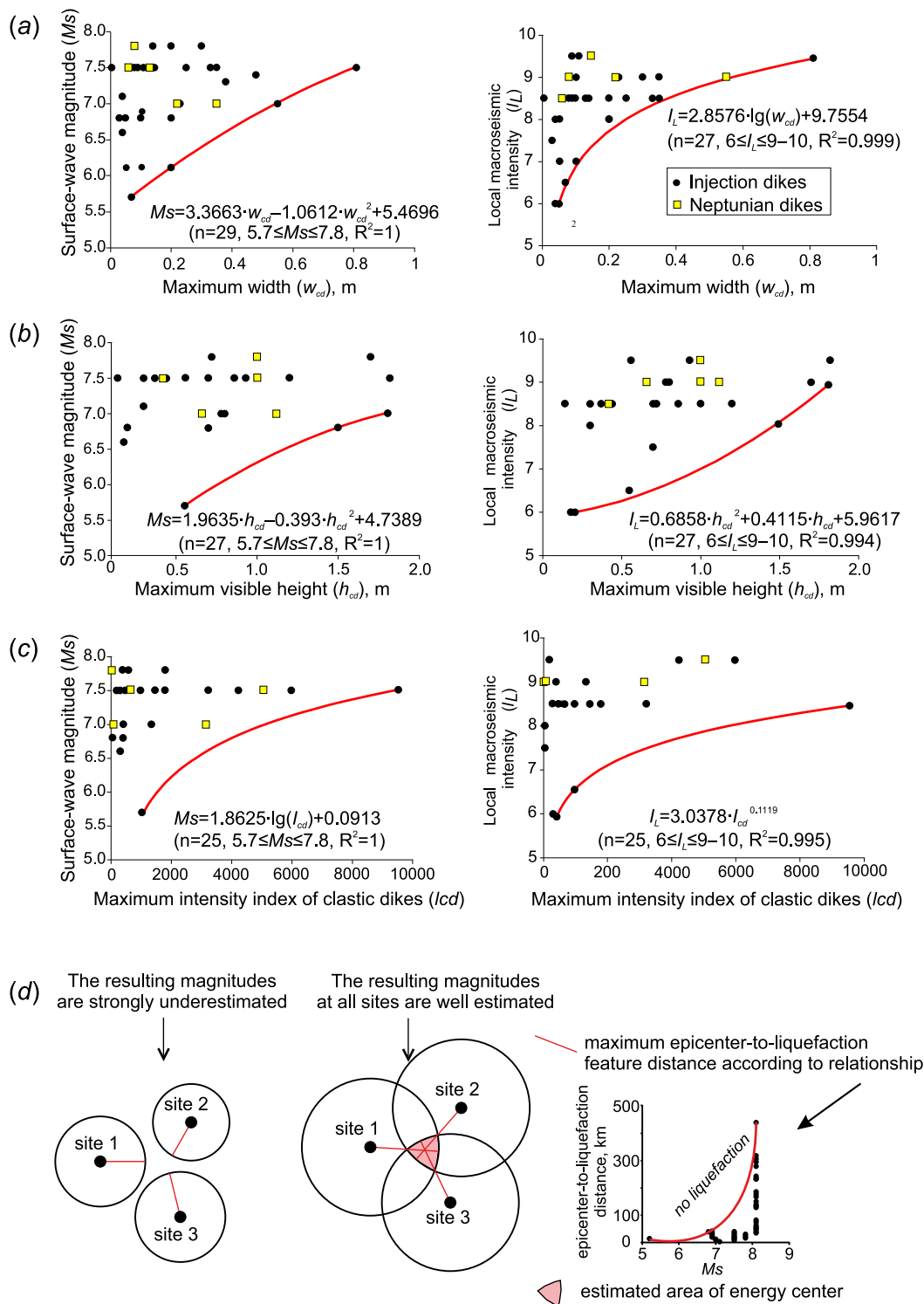


Fig. 12. (a–c) – bounding curves and upper-bound relationships of the earthquake magnitude (M_s) and the local macroseismic intensity at a site on MSK-64 intensity scale (I_L) vs. the dike parameters: (a) – maximum width (w_{cd}); (b) – maximum visible height (h_{cd}); (c) – maximum intensity index (I_{cd}). R^2 represents the determination coefficient, n – number of sites. (d) – a simple model to verify the estimated magnitude using the relationships of the epicenter-to-liquefaction feature distance vs. the earthquake magnitude after [Lunina, Gladkov, 2015].

Рис. 12. Граничные кривые, отражающие связь магнитуды (M_s) и интенсивности (I_L) в пункте по макросейсмической шкале MSK-64 с параметрами кластических даек: (a) – максимальной мощностью (w_{cd}); (b) – максимальной видимой высотой (h_{cd}); (c) – максимальным индексом интенсивности (I_{cd}). R^2 – коэффициент детерминации, n – количество точек наблюдения, в которых изучены дайки. (d) – упрощенная модель для проверки неопределенности в оценке M_s землетрясения с использованием известных уравнений связи между магнитудой и эпицентральной расстоянием от пунктов с наблюдаемыми одновозрастными дайками, возникшими в результате сейсмического разжижения по [Lunina, Gladkov, 2015].

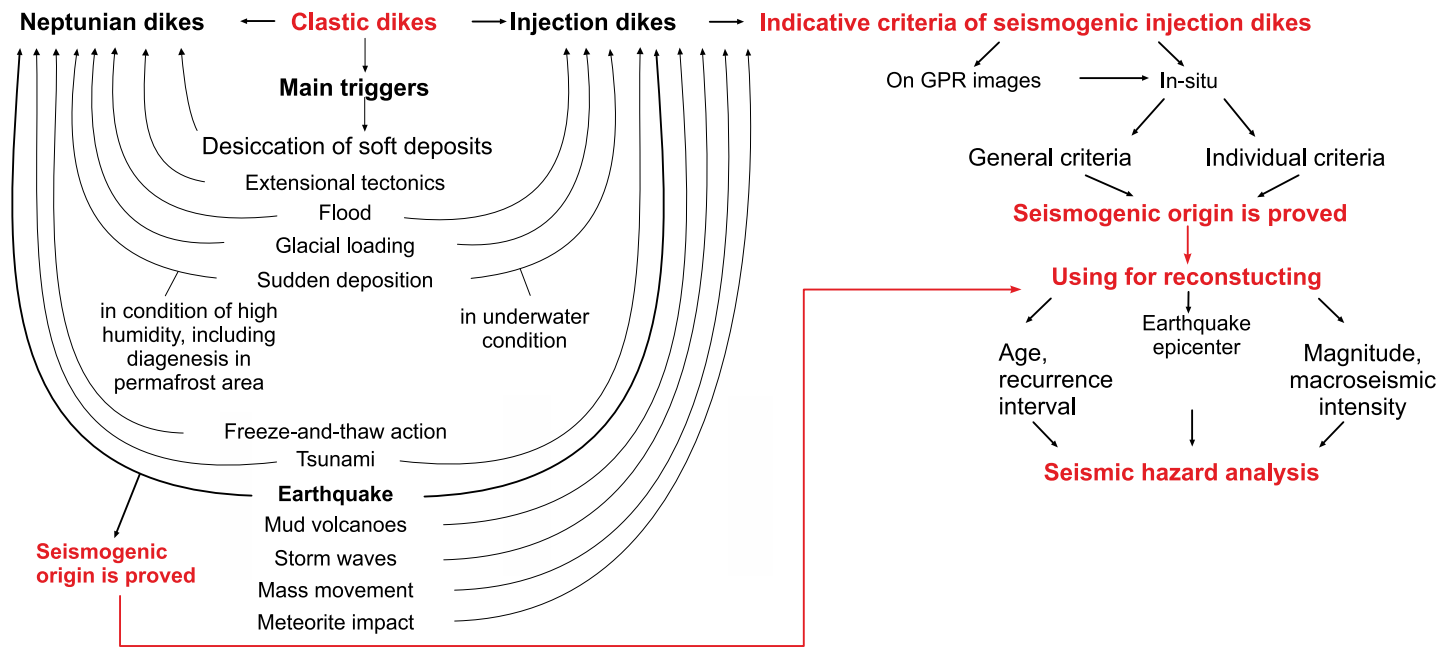


Fig. 13. General scheme showing a way to involve data on seismically induced clastic dikes in seismic hazard analysis.

Рис. 13. Обобщающая схема, показывающая путь вовлечения данных по нептуническим и инъекционным дайкам в анализ сейсмической опасности.

are high, and for all of the uncertainties of the equations, the real value of the dependent magnitude or intensity was equal to or larger than the calculated magnitude or intensity. The analysis of the obtained relationships showed that to estimate the lowest potential magnitude of a seismic event or local macroseismic intensity using clastic dikes, it is better to use all three parameters and take the maximum level for a seismic hazard evaluation [Lunina, Gladkov, 2015]. This is because that in most cases a geologist does not know if he measures maximum value of a structure. Thus, 63 % of clastic dikes from analyzed data set have widths ≤ 0.2 m (Fig. 12, a), which is typical of seismically induced injections [Obermeier et al., 2005; Levi et al., 2011].

In contrast to the width, the height of clastic dikes is not always consistent because we often do not see the region in which the initial bedding has been liquefied. The maximum visible height in author's data set of instrumental earthquakes is 1.82 m (Fig. 12, b), whereas the dikes in the epicentral area of historical 1811–1812 New Madrid, USA earthquakes with $M_w=7-8$ were 8 m high [Obermeier et al., 2005]. Nevertheless, the relationships between the earthquake parameters and the visible height of clastic dikes will be particularly effective in the case of revealing the narrow-width dikes that are much more common in the epicentral areas of earthquakes.

The relationships between the magnitude/local macroseismic intensity and the intensity index of clastic dikes should compensate seemingly for the missing maximum values of the height and width of clastic

dikes (Fig. 12, c). However, the analysis of the data set shows that they will be effective only in the case of several dikes in a sectional view. For a single dike in a trench, M_s and I_L obtained on I_{cd} parameter will be strongly underestimated, therefore it is better to apply the width and height values.

The relationships (Fig. 12) has limitations because it results in a lower-bound evaluation of seismological parameters. They do not consider the geotechnical conditions at the sites, epicentral distance and earthquake depths. Nevertheless, in the areas where surface ruptures on flat areas are difficult to recognize after decades because of erosional truncation, these equations can be very practical. Moreover, to apply the relationships of the epicenter-to-liquefaction feature distance versus earthquake magnitude (e.g., [Galli, 2000; Pappathanassiou et al., 2005; Castilla, Audemard, 2007; Lunina et al., 2014]) for at least three cases associated with the same seismic event, it is possible to verify its estimated value and even to constrain the area of the energy center that initiated the formation of the injection dikes (Fig. 12, d).

7. CONCLUSIONS

This brief overview considers the most recent advances in study of seismically induced clastic dikes, the data of which are important in seismic hazard analysis (Fig. 13). With a large variety of origins of soft-sediment deformations, tabular injections caused by fluidi-

zation from seismic liquefaction are the most reliable indicators of paleoseismicity in comparative with Neptunian dikes. At the same time, if the earthquake origin of the latter is proved, they can also be used for estimations of epicenter, age, magnitude and local macroseismic intensity of paleoseismic events. The main results of this summary are as follows:

1. Main triggers, formation mechanisms and some matching indicative features of Neptunian and injection dikes, including tabular and cylindrical bodies are systematized. The desiccation of unconsolidated deposits, extensional tectonics, flood, glacial loading, sudden deposition in underwater condition or in conditions of high humidity, including diagenesis in permafrost area, freeze-and-thaw action, tsunami, earthquake, inflow of fluid-generating clays in the region of high temperatures and overpressures and subsequent fracturing (mud volcanoes), storm waves, mass movement, and meteorite impact can initiate the development of these soft-sediment deformations. Some of the triggers result in both types of dikes, among which the injection ones are the most perspective in the paleoseismic tasks.

2. Based on the revision of known liquefaction features and specific descriptions of the injection dikes, 12 general and 12 individual geological and structural criteria, which make it possible to establish confidently their earthquake origin, are represented. Recommendations for use of these criteria, part of which may not be visible or obscured by superimposed exogenous processes are given. Even several criteria if supported by structural analysis compared to tectonic framework are significant to conclude seismic genesis of injection dikes. Additionally, indicative searching features of the injection dikes on GPR images are suggested.

3. The clastic dikes can be applied to determine the age and the recurrence interval, the epicenter location and a lower-bound magnitude/intensity of paleoearthquakes, thus providing geological data for seismic hazard assessments in the regions, in which unconsolidated deposits capable to liquefaction are common.

In the future, to develop approaches for studying paleoseismicity based on soft-sediment deformation structures, it is necessary to carry out specialized research in the epicentral zones of recent and well-documented historical seismic events in order to describe the geometry, morphology, composition of the dikes, as well as geological, geomorphological and hydrogeological conditions of their formation. Developing the bounding relationships between the parameters of clastic dikes and associated earthquakes, including the peak ground acceleration (PGA) would become perspective.

8. ACKNOWLEDGMENTS

The authors would like to express their gratitude to the Institute of the Earth's Crust, Siberian Branch of the Russian Academy of Sciences for providing the laboratory to carry out this research within a Base Budget Project 346-2016-0004. The author is also grateful to A. Gladkov for many years of fruitful cooperation and joint research of clastic dikes and liquefaction features in different regions of Siberia, as well as to I. Denisenko for participation in elaboration of GPR data. Special thanks to A.M. Korzhenkov and E.V. Deev whose productive comments and criticism improved the original manuscript.

9. REFERENCES

- Alexeev S., Alexeeva L., Kononov A., 2014. Cryogenic deformation structures in Late Cenozoic unconsolidated sediments of the Tunka depression in the Baikal Rift Zone. *Permafrost and Periglacial Process* 15 (2), 117–126. <https://doi.org/10.1002/ppp.1809>.
- Alfaro P., Delgado J., Estevez A., Molina J.M., Moretti M., Soria J.M., 2002. Liquefaction and fluidization structures in Messinian storm deposits (Bajo Segura Basin, Betic Cordillera, southern Spain). *International Journal of Earth Sciences* 91 (3), 505–513. <https://doi.org/10.1007/s00531-001-0241-z>.
- Al-Shukri H.J., Mahdi H., Tuttle M., 2006. Three-dimensional imaging of earthquake-induced liquefaction features with ground penetrating radar near Marianna, Arkansas. *Seismological Research Letters* 77 (4), 505–513. <https://doi.org/10.1785/gssrl.77.4.505>.
- Ambraseys N.N., 1988. Engineering Seismology. *Earthquake Engineering and Structural Dynamics* 17 (1), 1–105. <https://doi.org/10.1002/eqe.4290170101>.
- Anand A., Jain A.K., 1987. Earthquakes and deformational structures (seismites) in Holocene sediments from the Himalayan-Andaman Arc, India. *Tectonophysics* 133 (1–2), 105–120. [https://doi.org/10.1016/0040-1951\(87\)90284-8](https://doi.org/10.1016/0040-1951(87)90284-8).
- Artushkov E.V., 1963a. About possibility of initiation and general regularities of development of the convective instability in sedimentary rocks. *Doklady AN SSSR* 153 (1), 162–165 (in Russian) [Артюшков Е.В. О возможности возникновения и общих закономерностях развития конвективной неустойчивости в осадочных породах // Доклады АН СССР. 1963. Т. 153. № 1. С. 162–165].
- Artushkov E.V., 1963b. Main forms of convective structures in sedimentary rocks. *Doklady AN SSSR* 153 (2), 412–415 (in Russian) [Артюшков Е.В. Основные формы конвективных структур в осадочных породах // Доклады АН СССР. 1963. Т. 153. № 2. С. 412–415].

- Audemard F.A., de Santis F., 1991. Survey of liquefaction structures induced by recent moderate earthquakes. *Bulletin of the International Association of Engineering Geology* 44 (1), 5–16. <https://doi.org/10.1007/BF02602705>.
- Baradello L., Accaino F., 2016. GPR and high resolution seismic integrated methods to understand the liquefaction phenomena in the Mirabello Village (earthquake ML 5.9, 2012). *Engineering Geology* 211, 1–6. <https://doi.org/10.1016/j.enggeo.2016.06.027>.
- Bezerra F.H.R., da Fonseca V.P., Filho F.P.L., 2001. Seismites: origin, criteria for identification and examples from the Quaternary record of Northeastern Brazil. *Pesquisas em Geociencias* 28 (2), 205–212. <https://doi.org/10.22456/1807-9806.20295>.
- Bonilla M.G., Lienkaemper J.J., 1991. Factors affecting the recognition of faults exposed in exploratory trenches. United States Geological Survey Bulletin, No. 1947, 54 p. <https://doi.org/10.3133/b1947>.
- Borchardt G., Mace N., 1992. Clastic dike as evidence for a major earthquake along the Northern Hayward fault in Berkeley. In: Proceedings of Second Conference on earthquake hazards in the Eastern San Francisco Bay area. California Department of Conservation. Division of Mines and Geology Special Publication, vol. 113, p. 143–151.
- Braccini E., de Boer W., Hurst A., Huuse A., Vigorito M., Templeton G., 2008. Sand injectites. *Oilfield Review* (Summer issue), 34–49.
- Bump J. D., 1951. The White River Badlands of South Dakota. In: Guide Book of Fifth Field conference of the Society of vertebral paleontology in Western South Dakota. Museum of Geology, South Dakota School of Mines and Technology, Rapid City, South Dakota, p. 35–46.
- Castilla R.A., Audemard F.A., 2007. Sand blows as a potential tool for magnitude estimation of pre-instrumental earthquakes. *Journal of Seismology* 11 (4), 473–487. <https://doi.org/10.1007/s10950-007-9065-z>.
- Chen J., Van Loon A.J., Han Z., Chough S.K., 2009. Funnel-shaped, breccia-filled clastic dykes in the Late Cambrian Chaomidian Formation (Shandong Province, China). *Sedimentary Geology* 221 (1–4), 1–6. <https://doi.org/10.1016/j.sedgeo.2009.09.006>.
- Cooley S., 2011. Bibliography of Clastic Dike Research. Version 12.2011. Available from: <http://gis4geomorphology.com/wp-content/uploads/2014/02/Cooley-2011-Bibliography-of-Clastic-Dike-Research.pdf> (last accessed 25.07.2018).
- Cooley S., 2015. *Clastic dikes of the Columbia Basin*. Available from: <https://www.skyecooley.com/single-post/2015/07/22/Clastic-Dikes-of-the-Columbia-Basin-1> (last accessed 25.10.2017).
- Cooley S.W., Pidduck B.K., Pogue K.R., 1996. Mechanism and timing of emplacement of clastic dikes in the Touchet Beds of the Walla Walla Valley, south-central Washington. In: Geological Society of America Abstracts with Programs, vol. 28 (5), p. 57.
- Cox R.T., Hill A.A., Larsen D., Holzer T., Forman S.L., Noce T., Gardner C., Morat J., 2007. Seismotectonic implications of sand blows in the southern Mississippi Embayment. *Engineering Geology* 89 (3–4), 278–299. <https://doi.org/10.1016/j.enggeo.2006.11.002>.
- Danilov I.D., 1972. Permafrost and pseudo-permafrost lensoid deformations in sedimentary rocks. In: A.I. Popov (Ed.), Problems of cryolithology, Issue 2. Moscow State University Publishing House, Moscow, p. 31–48 (in Russian) [Данилов И.Д. Мерзлотные и псевдомерзлотные клиновидные деформации в осадочных породах // Проблемы криолитологии. Вып. 2 / Ред. А.И. Попов. М.: Изд-во МГУ, 1972. С. 31–48].
- Darwin C.R., 1846. Geological Observations on South America. Being the Third Part of the Geology of the Voyage of the Beagle, Under the Command of Capt. Fitzroy R.N. During the Years 1832–1836. Smith Elder and Co., London, 337 p. Available from: http://darwin-online.org.uk/converted/pdf/1846_SouthAmerica_F273.pdf (last accessed 25.07.2018).
- Deev E.V., Zolnikov I.D., Gus'kov S.A., 2009. Seismites in Quaternary sediments of southeastern Altai. *Russian Geology and Geophysics* 50 (6), 703–722. <https://doi.org/10.1016/j.rgg.2008.10.004>.
- Deev E.V., Zolnikov I.D., Lobova E.Yu., 2015. Late Pleistocene – Holocene coseismic deformations in the Malyi Yaloman River Valley (Gorny Altai). *Russian Geology and Geophysics* 56 (9), 1256–1272. <https://doi.org/10.1016/j.rgg.2015.08.003>.
- Dionne J.C., Shilts W.W., 1974. A Pleistocene clastic dike, upper Chaudiere valley, Quebec. *Canadian Journal of Earth Sciences* 11 (11), 1594–1605. <https://doi.org/10.1139/e74-158>.
- Ewertowski M., 2009. Ice-wedge pseudomorphs and frost-cracking structures in Weichselian sediments, Central-West Poland. *Permafrost and Periglacial Processes* 20 (4), 316–330. <https://doi.org/10.1002/ppp.657>.
- Fecht K.R., Lindsey K.A., Bjornstad B.N., Horton D.G., Last G.V., Reidel S.P., 1999. Clastic injection dikes of the Pasco Basin and vicinity. Bechtel Hanford Inc. Report, BHI-01103, 217 p. Available from: <https://www.nrc.gov/docs/ML0901/ML090120243.pdf> (last accessed 11.09.2018).
- Feng Z.-Z., 2017. A brief review on 7 papers from the special issue of “The environmental significance of soft-sediment deformation” of the *Sedimentary Geology* 344 [2016]. *Journal of Palaeogeography* 6 (4), 243–250. <https://doi.org/10.1016/j.jop.2017.07.001>.
- Galli P., 2000. New empirical relationships between magnitude and distance for liquefaction. *Tectonophysics* 324 (3), 169–187. [https://doi.org/10.1016/S0040-1951\(00\)00118-9](https://doi.org/10.1016/S0040-1951(00)00118-9).

- Garetsky R.G., 1956. Clastic dikes. *Izvestiya AN SSSR, seriya geologicheskaya* (3), 81–103 (in Russian) [Гапецкий Р.Г. Кластические дайки // Известия АН СССР, серия геологическая. 1956. № 3. С. 81–103].
- Gileva N.A., Mel'nikova V.I., Radziminovich N.A., Déverchère J., 2000. Location of earthquakes and average parameters of the crust in some areas of the Baikal region. *Geologiya i Geofizika (Russian Geology and Geophysics)* 41 (5), 609–615.
- Goździk J., van Loon A.J., 2007. The origin of a giant downward directed clastic dyke in a kame (Belchatów mine, central Poland). *Sedimentary Geology* 193 (1–4), 71–79. <https://doi.org/10.1016/j.sedgeo.2006.02.008>.
- Greb S.F., Dever G.R., 2002. Critical evaluation of possible seismites: examples from the Carboniferous of the Appalachian basin. In: F.R. Etensohn, N. Rast, C.E. Brett (Eds.), *Ancient seismites*. Geological Society of America Special Paper, vol. 359, p. 109–125. <https://doi.org/10.1130/0-8137-2359-0.109>.
- Green R.A., Obermeier S.F., Olson S.M., 2005. Engineering geologic and geotechnical analysis of paleoseismic shaking using liquefaction effects: field examples. *Engineering Geology* 76 (3–4), 263–293. <https://doi.org/10.1016/j.enggeo.2004.07.026>.
- Hargitai H., Levi T., 2015. Clastic dike. In: H. Hargitai, Á. Kereszturi (Eds.), *Encyclopedia of Planetary Landforms*. Springer Science+Business Media, New York, p. 307–313.
- Hsu C.-C., Lee D.-H., Ku C.-S., 2005. A case investigation of liquefaction features in a Coastal industrial park by using ground penetrating radar. In: *The Fifteenth International Offshore and Polar Engineering Conference*. Seoul, Korea. International Society of Offshore and Polar Engineers Publisher, p. 1–6.
- Ito M., Ishimoto S., Ito K., Kotake N., 2016. Geometry and lithofacies of coarse-grained injectites and extrudites in a late Pliocene trench-slope basin on the southern Boso Peninsula, Japan. *Sedimentary Geology* 344, 336–349. <https://doi.org/10.1016/j.sedgeo.2016.02.015>.
- Iverson R.M., George D.L., Allstadt K., Reid M.E., Collins B.D., Vallance J.W., Schilling S.P., Godt J.W., Cannon C.M., Magirl C.S., Baum R.L., Coe J.A., Schulz W.H., Bower J.B., 2015. Landslide mobility and hazards: implications of the 2014 Oso disaster. *Earth and Planetary Science Letters* 412, 197–208. <https://doi.org/10.1016/j.epsl.2014.12.020>.
- Jacoby Y., Weinberger R., Levi T., Marco S., 2015. Clastic dikes in the Dead Sea basin as indicators of local site amplification. *Natural Hazards* 75 (2), 1649–1676. <https://doi.org/10.1007/s11069-014-1392-0>.
- Jenkins O.P., 1925. Clastic dikes of Eastern Washington and their geologic significance. *American Journal of Science* 10 (57), 234–246. <https://doi.org/10.2475/ajs.s5-10.57.234>.
- Jolly R.J.H., Lonergan L., 2002. Mechanisms and controls on the formation of sand intrusions. *Journal of the Geological Society* 159 (5), 605–617. <https://doi.org/10.1144/0016-764902-025>.
- Jonk R., Duranti D., Parnell J., Hurst A., Fallick A.E., 2003. The structural and diagenetic evolution of injected sandstones: examples from the Kimmeridgian of NE Scotland. *Journal of the Geological Society* 160 (6), 881–894. <https://doi.org/10.1144/0016-764902-091>.
- Kholodov V.N., 1978. Sandy diapirism: a new aspect of catagenetic processes. Communication 1. Morphology, composition, and formation conditions of dikes and “horizons with inclusions” in the Miocene of the Eastern Cis-Caucasus. *Litologiya i Poleznye Iskopayemye (Lithology and Mineral Resources)* (4), 50–66 (in Russian) [Холодов В.Н. Песчаный диапиризм – новая сторона катагенетических процессов. Сообщение I. Морфология, состав и условия образования песчаных даек и “горизонтов с включениями” в миоцене Восточного Предкавказья // Литология и полезные ископаемые. 1978. № 4. С. 50–66].
- Kholodov V.N., 2002. Mud volcanoes: distribution regularities and genesis (Communication 2. Geological–geochemical peculiarities and formation model). *Lithology and Mineral Resources* 37 (4), 293–310. <https://doi.org/10.1023/A:1019955921606>.
- Korzhenkov A.M., Avanesian M.A., Karakhanian A.S., Virgino A., 2014. Seismic convolutions in the Quaternary deposits of Lake Sevan, Armenia. *Russian Geology and Geophysics* 55 (1), 46–53. <https://doi.org/10.1016/j.rgg.2013.12.003>.
- Kostyaev A.G., 1969. Diagenetic wedge forms in recent alluvial sediments of the Nizhny Omoloi River basin. In: A.I. Popov (Ed.), *Problems of cryolithology*, Issue 1. Moscow State University Publishing House, Moscow, p. 63–79 (in Russian) [Костяев А.Г. Диагенетические клиновидные формы в современных аллювиальных отложениях бассейна Нижнего Омолая // Проблемы криолитологии. Вып. 1 / Ред. А.И. Попов. М.: Изд-во МГУ, 1969. С. 63–79].
- Kring D.A., Hörz F., Zurcher L., Fucugauchi U., 2004. Impact lithologies and their emplacement in the Chicxulub impact crater: initial results from the Chicxulub Scientific Drilling Project, Yaxcopoil, Mexico. *Meteoritics & Planetary Science* 39 (6), 879–897. <https://doi.org/10.1111/j.1945-5100.2004.tb00936.x>.
- Kuribayashi E., Tatsuoka F., 1975. Brief review of liquefaction during earthquakes in Japan. *Soils and Foundations* 15 (4), 81–92. https://doi.org/10.3208/sandf1972.15.4_81.
- Larsen E., Mangerud J., 1992. Subglacially formed clastic dikes. *Sveriges Geologiska Undersökning, series Ca* 81, 163–170.
- Le Roux J.P., Nielsen S.N., Kemnitz H., Henriquez Á., 2008. Pliocene mega-tsunami deposit and associated features in the Ranquil Formation, southern Chile. *Sedimentary Geology* 203 (1–2), 164–180. <https://doi.org/10.1016/j.sedgeo.2007.12.002>.
- Levi T., Weinberger R., Aifa T., Eyal Y., Marco S., 2006. Injection mechanism of clay-rich sediments into dikes during earthquakes. *Geochemistry, Geophysics, Geosystems* 7 (12), Q12009. <https://doi.org/10.1029/2006GC001410>.

- Levi T., Weinberger R., Eyal Y., 2009. Decay of dynamic fracturing based on three-dimensional measurements of clastic-dike geometry. *Journal of Structural Geology* 31 (8), 831–841. <https://doi.org/10.1016/j.jsg.2009.06.002>.
- Levi T., Weinberger R., Eyal Y., 2011. A coupled fluid-fracture approach to propagation of clastic dikes during earthquakes. *Tectonophysics* 498 (1–4), 35–44. <https://doi.org/10.1016/j.tecto.2010.11.012>.
- Li Y., Craven J., Schweig E.S., Obermeier S.F., 1996. Sand boils induced by the 1993 Mississippi River flood: could they one day be misinterpreted as earthquake induced liquefaction? *Geology* 24 (2), 171–174. [https://doi.org/10.1130/0091-7613\(1996\)024<0171:SBIBTM>2.3.CO;2](https://doi.org/10.1130/0091-7613(1996)024<0171:SBIBTM>2.3.CO;2).
- Liu L., Li Y., 2001. Identification of liquefaction and deformation features using ground penetrating radar in the New Madrid seismic zone, USA. *Journal of Applied Geophysics* 47 (3–4), 199–215. [https://doi.org/10.1016/S0926-9851\(01\)00065-9](https://doi.org/10.1016/S0926-9851(01)00065-9).
- Liu Y., Xie J.F., 1984. Seismic liquefaction of sand. Earthquake Press, Beijing, China (in Chinese).
- Lunina O.V., Andreev A.V., Gladkov A.A., 2014. Geological hazards associated with seismogenic faulting in southern Siberia and Mongolia: forms and location patterns. *Russian Geology and Geophysics* 55 (8), 1017–1031. <https://doi.org/10.1016/j.rgg.2014.07.010>.
- Lunina O.V., Andreev A.V., Gladkov A.S., 2012. The Tsagan earthquake of 1862 on Lake Baikal revisited: a study of secondary coseismic soft-sediment deformation. *Russian Geology and Geophysics* 53 (6), 571–587. <https://doi.org/10.1016/j.rgg.2012.04.007>.
- Lunina O.V., Andreev A.V., Gladkov A.S., 2015. The 1950 Mw=6.9 Mondy earthquake in southern East Siberia and associated deformations: facts and uncertainties. *Journal of Seismology* 19 (1), 171–189. <https://doi.org/10.1007/s10950-014-9457-9>.
- Lunina O.V., Gladkov A.S., 2015. Seismically induced clastic dikes as a potential approach for the estimation of the lower-bound magnitude/intensity of paleoearthquakes. *Engineering Geology* 195, 206–213. <https://doi.org/10.1016/j.enggeo.2015.06.008>.
- Lunina O.V., Gladkov A.S., 2016. Soft-sediment deformation structures induced by strong earthquakes in southern Siberia and their paleoseismic significance. *Sedimentary Geology* 344, 5–19. <https://doi.org/10.1016/j.sedgeo.2016.02.014>.
- Lupher R.L., 1944. Clastic dikes of the Columbia Basin region, Washington and Idaho. *Geological Society of America Bulletin* 55 (12), 1431–1462. <https://doi.org/10.1130/GSAB-55-1431>.
- McCalpin J.P. (Ed.), 2009. Paleoseismology. 2nd edition. Elsevier, Amsterdam, 613 p.
- McNulty W.E., Obermeier S.F., 1997. Liquefaction evidence for at least two strong Holocene paleo-earthquakes in central and southwestern Illinois, USA. U.S. Geological Survey Open-File Report 97-435, 22 p. Available from: <https://pubs.usgs.gov/of/1997/0435/report.pdf> (last accessed 25.07.2018).
- Montenat C., Barrier P., d'Estevou P., 1991. Some aspects of the recent tectonics in the Strait of Messina, Italy. *Tectonophysics* 194 (3), 203–215. [https://doi.org/10.1016/0040-1951\(91\)90261-P](https://doi.org/10.1016/0040-1951(91)90261-P).
- Montenat C., Barrier P., d'Estevou P.O., Hibsich C., 2007. Seismites: An attempt at critical analysis and classification. *Sedimentary Geology* 196 (1–4), 5–30. <https://doi.org/10.1016/j.sedgeo.2006.08.004>.
- Moretti M., Alfaro P., Caselles O., Canas, J.A., 1999. Modelling seismites with a digital shaking table. *Tectonophysics* 304 (4), 369–383. [https://doi.org/10.1016/S0040-1951\(98\)00289-3](https://doi.org/10.1016/S0040-1951(98)00289-3).
- Moretti M., Sabato L., 2007. Recognition of trigger mechanisms for soft-sediment deformation in the Pleistocene lacustrine deposits of the Sant'Arcangelo Basin (Southern Italy): Seismic shock vs. Overloading. *Sedimentary Geology* 196 (1–4), 31–45 <https://doi.org/10.1016/j.sedgeo.2006.05.012>.
- Newsom J.F., 1903. Clastic dikes. *Bulletin of the Geological Society of America* 14 (1), 227–268. <https://doi.org/10.1130/GSAB-14-227>.
- Nobes D.C., Bastin S., Charlton G., Cook R., Gallagher M., Graham H., Grose D., Hedley J., Scott Sharp-Heward S., Templeton S., 2013. Geophysical imaging of subsurface earthquake-induced liquefaction features at Christchurch Boys High School, Christchurch, New Zealand. *Journal of Environmental & Engineering Geophysics* 18 (4), 255–267. <https://doi.org/10.2113/JEEG18.4.255>.
- Novikov I., Vapnik Y., Safonova I., 2013. Mud volcano origin of the Mottled Zone, South Levant. *Geoscience Frontiers* 4 (5), 597–619. <https://doi.org/10.1016/j.gsf.2013.02.005>.
- Obermeier S.F., 1996. Use of liquefaction-induced features for paleoseismic analysis – An overview of how seismic liquefaction features can be distinguished from other features and how their regional distribution and properties of source sediment can be used to infer the location and strength of Holocene paleo-earthquakes. *Engineering Geology* 44 (1–4), 1–76. [https://doi.org/10.1016/S0013-7952\(96\)00040-3](https://doi.org/10.1016/S0013-7952(96)00040-3).
- Obermeier S.F., 1998. Liquefaction evidence for strong earthquakes of Holocene and Latest Pleistocene ages in the states of Indiana and Illinois, USA. *Engineering Geology* 50 (3–4), 227–254. [https://doi.org/10.1016/S0013-7952\(98\)00032-5](https://doi.org/10.1016/S0013-7952(98)00032-5).
- Obermeier S.F., Olson S.M., Green R.A., 2005. Field occurrences of liquefaction-induced features: a primer for engineering geologic analysis of paleoseismic shaking. *Engineering Geology* 76 (3–4), 209–234. <https://doi.org/10.1016/j.enggeo.2004.07.009>.

- Onorato M.R., Perucca L., Coronato A., Rabassa J., López R., 2016. Seismically-induced soft-sediment deformation structures associated with the Magallanes – Fagnano Fault System (Isla Grande de Tierra del Fuego, Argentina). *Sedimentary Geology* 344, 135–144. <https://doi.org/10.1016/j.sedgeo.2016.04.010>.
- Owen G., Moretti M., 2011. Identifying triggers for liquefaction-induced soft-sediment deformation in sands. *Sedimentary Geology* 235 (3–4), 141–147. <https://doi.org/10.1016/j.sedgeo.2010.10.003>.
- Owen G., Moretti M., Alfaro P., 2011. Recognising triggers for soft-sediment deformation: Current understanding and future directions. *Sedimentary Geology* 235 (3–4), 133–140. <https://doi.org/10.1016/j.sedgeo.2010.12.010>.
- Papadopoulos A.G., Lefkopoulos G., 1993. Magnitude – distance relation for liquefaction in soil from earthquakes. *Bulletin of the Seismological Society of America* 83 (3), 925–938.
- Papathanassiou G., Pavlides S., Christaras B., Pitilakis K., 2005. Liquefaction case histories and empirical relations [of earthquake magnitude versus distance from the boarder Aegean region. *Journal of Geodynamics* 40 (2–3), 257–278. <https://doi.org/10.1016/j.jog.2005.07.007>.
- Passchier S., 2000. Soft-Sediment deformation features in core from CRP-2/2A, Victoria Land basin, Antarctica. *Terra Antarctica* 7 (3), 401–412.
- Porat N., Levi T., Weinberger R., 2007. Possible resetting of quartz OSL signals during earthquakes – evidence from late Pleistocene injection dikes, Dead Sea basin, Israel. *Quaternary Geochronology* 2 (1–4), 272–277. <https://doi.org/10.1016/j.quageo.2006.05.021>.
- Quigley M.C., Bastin S., Bradley B.A., 2013. Recurrent liquefaction in Christchurch, New Zealand, during the Canterbury earthquake sequence. *Geology* 41 (4), 419–422. <https://doi.org/10.1130/G33944.1>.
- Rodríguez-Pascua M.A., Silva P.G., Perucha M.A., Giner-Robles J.L., Heras C., Bastida A.B., Carrasco P., Roquero E., Lario J., Bardaji T., Pérez-López R., Elez J., 2016. Seismically induced liquefaction structures in La Magdalena archaeological site, the 4th century AD Roman Complutum (Madrid, Spain). *Sedimentary Geology* 344, 34–46. <https://doi.org/10.1016/j.sedgeo.2016.01.025>.
- Rogozhin E.A., 2012. Essays in Regional Seismotectonics. IPE RAS, Moscow, 340 p. (in Russian) [Рогожин Е.А. Очерки региональной сейсмотектоники. М.: ИФЗ РАН, 2012. 340 с.].
- Rossetti D.F., 1999. Soft-sediment deformation structures in Late Albian to Cenomanian deposits, São Luís Basin, Northern Brazil: evidence for palaeoseismicity. *Sedimentology* 46 (6), 1065–1081. <https://doi.org/10.1046/j.1365-3091.1999.00265.x>.
- Rusakov A.V., Nikonov A.A., 2010. Characterization of relict Late Pleistocene and Early Holocene paleosols buried in wedge-shaped structures on the southern coast of the Finnish Gulf. *Eurasian Soil Science* 43 (7), 737–747. <https://doi.org/10.1134/S1064229310070033>.
- Saucier R.T., 1989. Evidence for episodic sand-blow activity during the 1811–12 New Madrid (Missouri) earthquake series. *Geology* 17 (2), 103–106. [https://doi.org/10.1130/0091-7613\(1989\)017<0103:EFESBA>2.3.CO;2](https://doi.org/10.1130/0091-7613(1989)017<0103:EFESBA>2.3.CO;2).
- Seilacher A., 1969. Fault-graded beds interpreted as seismites. *Sedimentology* 13 (1–2), 155–159. <https://doi.org/10.1111/j.1365-3091.1969.tb01125.x>.
- Seilacher A., 1991. Events and their signatures – an overview. In: G. Einsele, W. Reiken, A. Seilacher (Eds.), *Cycles and events in stratigraphy*. Springer, Berlin, p. 222–226.
- Shanmugan G., 2016. The seismite problem. *Journal of Palaeogeography* 5 (4), 318–362. <https://doi.org/10.1016/j.jop.2016.06.002>.
- Shanmugan G., 2017. Global case studies of soft-sediment deformation structures (SSDS): Definitions, classifications, advances, origins, and problems. *Journal of Palaeogeography* 6 (4), 251–320. <https://doi.org/10.1016/j.jop.2017.06.004>.
- Shrock B.R., 1948. *Sequence in Layered Rocks*. Mc Graw-Hill, New York, 507 p.
- Sims J.D., 1975. Determining earthquake recurrence intervals from deformational structures in young lacustrine sediments. *Tectonophysics* 29 (1–4), 141–152. [https://doi.org/10.1016/0040-1951\(75\)90139-0](https://doi.org/10.1016/0040-1951(75)90139-0).
- Sims J.D., Garvin C.D., 1995. Recurrent liquefaction induced by the 1989 Loma Prieta earthquake and 1990 and 1991 aftershocks: implications for paleoseismicity studies. *Bulletin of the Seismological Society of America* 85 (1), 51–65.
- Spencer P.K., Jaffee P.K., 2002. Pre-Late Wisconsinan glacial outburst floods in Southeastern Washington – The indirect Record. *Washington Geology* 30 (1–2), 9–16.
- Srtangways W.T.H.F., 1821. Geological sketch of the Environs of Petersburg. *Transactions of the Geological Society of London* 5, 392–458.
- Talwani P., Hasek M., Gassman S., Doar W.R., Chapman A., 2011. Discovery of a sand blow and associated fault in the epicentral area of the 1886 Charleston Earthquake. *Seismological Research Letters* 82 (4), 589–598. <https://doi.org/10.1785/gssrl.82.4.589>.
- Tuttle M.R., 2001. The use of liquefaction features in paleoseismology: Lessons learned in the New Madrid seismic zone, central United States. *Journal of Seismology* 5 (3), 361–380. <https://doi.org/10.1023/A:1011423525258>.
- Van Loon A.J., 2014. The life cycle of seismite research. *Geologos* 20 (2), 61–66. <https://doi.org/10.2478/logos-2014-0005>.

- Van Loon A.J., Maulik P., 2011. Abraded sand volcanoes as a tool for recognizing paleo-earthquakes, with examples from the Cisuralian Talchir Formation near Angul (Orissa, eastern India). *Sedimentary Geology* 238 (1–2), 145–155. <https://doi.org/10.1016/j.sedgeo.2011.04.009>.
- Van Vliet-Lanoë B., Magyari A., Meilliez F., 2004. Distinguishing between tectonic and periglacial deformations of quaternary continental deposits in Europe. *Global and Planetary Change* 43 (1–2), 103–127. <https://doi.org/10.1016/j.gloplacha.2004.03.003>.
- Vanneste K., Meghraoui M., Camelbeeck T., 1999. Late Quaternary earthquake-related soft-sediment deformation along the Belgian portion of the Feldbiss Fault, Lower Rhine Graben system. *Tectonophysics* 309 (1–4), 57–79. [https://doi.org/10.1016/S0040-1951\(99\)00132-8](https://doi.org/10.1016/S0040-1951(99)00132-8).
- Wakamatsu K., 1993. History of soil liquefaction in Japan and assessment of liquefaction potential based on geomorphology. A Thesis in the Department of Architecture Presented in Partial Fulfillment of the Requirements for the Degree of Doctor of Engineering, Waseda University, Tokyo, Japan, 245 p.
- Wheeler R.L., 2002. Distinguishing seismic from nonseismic soft-sediment structures: Criteria from seismic-hazard analysis. In: F.R. Ethensohn, N. Rast, C.E. Brett (Eds.), *Ancient seismites*. Geological Society of America Special Papers, vol. 359, p. 1–11. <https://doi.org/10.1130/0-8137-2359-0.1>.
- Youd T.L., 1973. Liquefaction, Flow, and Associated Ground Failure. US Geological Survey Circular 688, 12 p. <https://doi.org/10.3133/cir688>.
- Youd T.L., Perkins D.M., 1978. Mapping of liquefaction induced ground failure potential. *Journal of the Geotechnical Engineering Division* 104 (4), 433–446.

INFORMATION ABOUT AUTHOR | СВЕДЕНИЯ ОБ АВТОРЕ

Oksana V. Lunina

Doctor of Geology and Mineralogy, Lead Researcher

Institute of the Earth's Crust, Siberian Branch of RAS
128 Lermontov street, Irkutsk 664033, Russia

✉ e-mail: lounina@crust.irk.ru

🆎 <https://orcid.org/0000-0001-7743-8877>

Оксана Викторовна Лунина

докт. геол.-мин. наук, в.н.с.

Институт земной коры СО РАН
664033, Иркутск, ул. Лермонтова, 128, Россия